Expressing human Orai3 in insect cells for pharmacological studies

A thesis submitted in partial fulfillment
of the requirements for the degree of
Master of Science

by

Orville R. Bennett
B.S., University of Hartford, 2005

2011
Wright State University

Wright State University
SCHOOL OF GRADUATE STUDIES

December 14, 2011

I HEREBY RECOMMEND THAT THE THESIS PREPARED UNDER MY SUPERVISION BY Orville R. Bennett ENTITLED Expressing human Orai3 in insect cells for pharmacological studies BE ACCEPTED IN PARTIAL FULFILLMENT OF THE REQUIREMENTS FOR THE DEGREE OF Master of Science.

J. Ashot Kozak, Ph. D.
Thesis Director

Timothy Cope, Ph. D.
Chair, Department of Neuroscience,
Cell Biology and Physiology

Committee on
Final Examination

J. Ashot Kozak, Ph. D.

Thomas Brown, Ph. D.

Adrian Corbett, Ph. D.

Robert Putnam, Ph. D.

Andrew Hsu, Ph.D.
Dean, School of Graduate Studies

ABSTRACT

Bennett, Orville. M.S., Department of Neuroscience, Cell Biology and Physiology, Wright State University, 2011. *Expressing human Orai3 in insect cells for pharmacological studies.*

The Orai3 protein, forms a Ca^{2+} channel with a pharmacological profile distinct from its close relative, the store-operated Ca^{2+} channel Orai1. Though closely related to Orai1, the function of Orai3 in humans is still unclear. This study attempts to contribute to the body of knowledge by undertaking a pharmacological analysis of Orai3 in insect cells. We describe here the creation of a vector capable of expressing the mammalian Orai3 gene on an insect background. We demonstrate the ability to induce gene expression of Orai3 in these insect cells, and then assess the effectiveness of this system by characterizing the pharmacological properties with the drug 2-Aminoethyl diphenylborinate (2-APB). The results show that the current strategy used to express Orai3 will require additional refinement before the system can be considered generally useful for pharmacological studies, because expression of Orai3 may be affected by native proteins. The interference of expression seems confined to Orai Ca^{2+} channels, as mammalian STIM1 was also expressed and a response to 2-APB, albeit unexpected, was observed.

Contents

List of Figures

List of Tables

Acknowledgement

I would like to extend my thanks to yada yada yada (maybe your parents?)

More thankful yada...

Even more yada...

Dedicated to

Laura Bennett. This one's fer you kid.

Introduction

In 1983, two events of note occurred; the first being my birth, and the second, the publishing of an article in Nature by Streb et al. (38) which showed that inositol(1,4,5)-trisphosphate (IP3) triggered the release of calcium (Ca^{2+}) from the endoplasmic reticulum (ER). A few years later, in 1986, Putney (31), proposed that depletion of $[Ca^{2+}]_i$ signaled the plasma membrane Ca^{2+} entry channels to open (39). This and other early studies (17, 49) formed the basis for what we now refer to as store-operated calcium entry (SOCE). Initially, the more popular term used was capacitative calcium entry (CCE). Over 20 years later, the other major players in this story came into the view. Stromal interaction molecule 1 (STIM1), was found to affect SOC influx in an RNA_i screen and identified as the ER calcium sensor (33, 22, 48). Shortly thereafter, Orai1 was found and identified as the store-operated calcium channel (29, 41, 14, 47, 36).

The mammalian Orai1 has two homologs, Orai2 and Orai3, whose functions have not yet been clarified (33, 41, 39, 36). It may be the case that the proteins encoded by these genes are expressed in a tissue-specific manner. This seems to be the case with estrogen receptor-positive (ER+) breast cancer cells, which have been shown to use Orai3 as their store-operated Ca^{2+} channel (10). The demonstrable involvement of Orai3 in a disease state as prevalent as breast cancer, underscores the importance of further studies of these Orai channels whose function in the body is not yet understood. The presented study sets the foundation for performing a pharmacological characterization of the Orai3 Ca^{2+} channel, by using *Drosophila* S2 cells as a heterologous expression system. This system

is expected to be of more general use for physiological and pharmacological studies of all Orai channels. We begin by introducing calcium signaling through store-operated channels in non-excitable cells.

1.1 Background

1.1.1 Calcium Signaling

Ultimately we will be looking at the effect which 2-APB has on Orai3, using cellular Ca^{2+} elevations as our output. Ca^{2+} is an incredibly versatile signaling molecule, affecting all parts of the cellular signaling machinery. Ca^{2+} signaling is critical to such processes as exocytosis, transcription, cardiac function, mitosis and apoptosis (4, 5, 16, 36). The speed of these processes range from seconds to minutes to days (4).

Orai3 is in the same family as Orai1 (14, 39, 16), the recently identified Calcium-Release Activated Calcium (CRAC) channel, and is thought to be related to store-operated calcium entry (SOCE). It is important then to understand the role that Ca^{2+} plays in this process. Cell calcium sources are both internal and external (4, 5, 36). It is necessary then, to maintain a balance between the two pathways, to prevent calcium from accumulating where it should not, thereby activating or deactivating cellular processes at inopportune times. The internal source of calcium we will be looking at is the endoplasmic reticulum (ER). The ER releases Ca^{2+} from its stores through Ca^{2+}-permeable channels, the most studied of them being the IP3 and ryanodine receptors (IP3R, RYR) (5, 6). These channels are in fact activated via second messengers. IP3R, for example, is activated by IP3 and this opens the channel releasing ER Ca^{2+} into the cytoplasm. IP3 is the soluble product of phosphatidylinositol(4,5)diphosphate (PIP2) cleavage by phospholipase C gamma (PLC_{γ}) in T-lymphocytes (5, 21).

"On" mechanisms are the means by which Ca^{2+} is released from internal stores into

the cytoplasm. "On" mechanisms depend on Ca^{2+} channels (5) which may be voltage-operated channels (VOCs), receptor-operated channels, and/or store-operated channels (SOCs) (5). Orai1 is a store-operated Ca^{2+} channel (29, 41, 14, 47, 36).

"Off" mechanisms also exist to quickly lower $[Ca^{2+}]_i$, and this is done through various pumps and exchangers (5). The plasma membrane Ca^{2+}-ATPase and Na^+/Ca^{2+} exchanger will move Ca^{2+} out of the cell, while the sarco-endoplasmic reticulum Ca^{2+} ATPase will pump Ca^{2+} back into the ER, replenishing the cell's internal stores (5).

When SOCs open they allow Ca^{2+} into the cytosol. This leads to $[Ca^{2+}]_i$ increasing from nanomolar to micromolar levels (5). Ca^{2+} is both stimulatory and inhibitory (5), since Ca^{2+} acts as a signal for such a wide array of cellular processes. Spatial regulation then, is very important, and serves as a way to control Ca^{2+}-dependent mechanisms. Ca^{2+}-binding proteins, which act as buffers, provide a way for the cell to control the local $[Ca^{2+}]_i$. Cytosolic Ca^{2+} buffers such as parvalbumin, calbindin-D, and calreticulin, (5) along with Ca^{2+} pumps and exchangers become important regulators of $[Ca^{2+}]_i$.

Cytosolic Ca^{2+} binding proteins are capable of more then buffering; they can also act as Ca^{2+} sensors (5). Ca^{2+} sensors, such as troponin C and calmodulin, respond to changes in $[Ca^{2+}]_i$. They do so with the aid four EF hand motifs and will bind Ca^{2+} to undergo conformational changes, and then activate downstream processes (5). This mechanism of detecting changes in $[Ca^{2+}]_i$ should be emphasized, as it will become relevant for another player in the SOCE mechanism, STIM1.

1.1.2 Store-Operated Calcium Entry

Store-operated calcium entry is an interesting, yet simple process. Broken down to its simplest form, it is merely a process which signals Ca^{2+} to enter the cell when it is in need of more Ca^{2+}(31, 5, 21). What triggers the process is the loss of Ca^{2+} from the cell's own internal Ca^{2+} stores. This increases the intracellular Ca^{2+} and allows for replenishing the stores (39), as well as providing Ca^{2+} necessary for various cellular processes (4, 5, 16, 36).

Store-operated Ca^{2+} channels in lymphocytes are responsible for Ca^{2+} entering from extracellular fluid (i.e. blood) (21, 5, 16). This sustained Ca^{2+} influx is necessary for gene transcription driven by nuclear factor of activated T-cells (NF-AT) (40, 5, 21, 16). NF-AT, a transcription factor, is activated when an immune response is necessary, and drives the transcription of IL-2 genes (40, 21, 16). The importance of Ca^{2+} to this process is a result of NF-AT's dependence on calcineurin for activation.

The Ca^{2+} release triggered by SOCE results in Ca^{2+} and calmodulin binding to calcineurin and activating it. Activated calcineurin then dephosphorylates NF-AT, allowing it to move into the nucleus (2). Once inside the nucleus, NF-AT is able to bind the promoter region of interleukin and proliferation genes enabling their transcription; in effect triggering immune response (40, 5, 16). Notice that for efficient NF-AT activation, the Ca^{2+} elevation needs to be sustained, for 1-2 hours (40, 5, 21).

Now that we have presented a general idea of SOCE it will hopefully be easier to understand the mechanism. T-cell receptor engagement activates the enzyme phospholipase C gamma (PLC_γ). PLC_γ will then hydrolyze phosphatidylinositol 4,5-bisphosphate (PIP2) resulting in soluble IP3, and membrane bound diacylglycerol (DAG) (5, 21). The IP3 binds to IP3 receptor (IP3R) opening it and allowing Ca^{2+} out of the ER down its concentration gradient (36, 39, 21). The decrease in *Drosophila* ER calcium is detected, and serves as a signal for extracellular Ca^{2+} flow in through the plasma membrane (PM) (36).

1.2 STIM1

Stromal interaction molecule 1 (STIM1), initially discovered as a transmembrane protein (42), was later shown to act as a sensor for Ca^{2+} within the ER (33, 22, 48, 36). The related STIM2 and *Drosophila* STIM (*dStim*) were also discovered (42).

STIM1 is able to function as a Ca^{2+} sensor due to its EF hand (42, 22), which is a motif also present in cytosolic Ca^{2+} sensors (see above). Upon depletion, ER-localized

STIM1 will migrate to sites at or near the plasma membrane and, through interactions with SOCE channels, will somehow help in activation of these channels. Once activated, channels in the Orai family - Orai1 being the only one which is both necessary and sufficient for Ca^{2+} entry - allow Ca^{2+} into the cell. STIM2, meanwhile, was found to be an inhibitor of STIM1-mediated SOCE (37). *dStim* while an important regulator of SOCE is also important in *Drosophila* developmentally (13). STIM1 and STIM2 are single-pass transmembrane proteins (16). Both are ER localized proteins, until emptying of the ER Ca^{2+} store causes translocation into, or close to, the plasma membrane (16).

1.3 Orai3

As mentioned previously, the Orai3 channel belongs to a family whose primary member, Orai1, has been identified as the long sought after store operated calcium (SOC) channel (14, 16). This is why studying Orai3 is important.

In this study we will seek to determine some properties of Orai3. In the mammalian system, a drug named 2-APB will, at low concentrations activate Orai1 but at higher concentrations inactivate it (14). 2-APB was shown to activate Orai3 at concentrations of 50 or 100 μM in the mammalian system however (46).

We already know some parts of the equation, but even now, years after its discovery, the field still has a poor understanding of Orai3's function. It is known that Orai3 can take part in interactions similar to that of Orai1. One of those, an interaction with the chemical 2-APB results in different cellular responses depending on the protein to which it binds. While Orai1 will see a slight activation upon introduction of < 30 μM amounts of 2-APB to its cellular milieu (15, 29), introduction of higher concentrations (> 30 μM) results in deactivation (15, 46), and blockade of SOCE. Orai3 on the other hand is activated by concentrations around 50 μM (15, 46). This is suggestive of direct interactions with 2-APB, which if true could help glean new information about Orai3 structure. If the interactions

are direct, crystal structures with 2-APB could help define the structure of this binding site, and lead to information helpful in finding the natural modulator of this SOCE activating function. It is evident then, that the question of whether Orai3 interacts directly with 2-APB is an important one.

The Orai family of proteins displays a wide expression profile, which includes T-cells and kidney (16). In HEK293 cells, knock down of Orai1 using siRNA reduced SOCE (16). Knock down of Orai2 or Orai3 did not significantly affect SOCE, however (16). These experiments in HEK cells are suggestive of Orai1's importance in initiating SOCE. As long as Orai1 is around, then SOCE takes place normally. Overexpression experiments of Orai1 showing Ca^{2+} influx for minutes support this idea (16, 46). Ca^{2+} influx on the order of hours is necessary for gene transcription however.

Expression of Orai3 and STIM1 in SCID T-cells results in marginal increases in SOCE, far lower than when Orai1 and STIM1 are overexpressed (16). In SCID patient fibroblast cells only Orai3 showed a minor increase in SOCE, over basal levels (16). Orai2 and STIM1 expression did not result in any increase over the basal SCID T-cell levels. These experiments indicate that while Orai2 and Orai3 are, at some level, capable of allowing SOCE, in these cell types they are not the primary mediators of SOCE.

These results may be taken to suggest that Orai3 is potentially important to SOCE in cell types that do not rely on Orai1 for sustained Ca^{2+} levels, as T-cells do. An example of this has been displayed for ER+ cancer cells. This shows that Orai3, by itself, is an important target of scientific inquiry, and that finding ways to ease its study is a relevant and valuable endeavor. In this study we begin this process by attempting to create a model system for studying pharmacological effects on Orai3.

1.4 *Drosophila* S2 cells

Drosophila cell line 2 (S2) has risen to prominence due to the ease of expressing proteins from other organisms in them. S2 cells have been used for both transient and stable expression of recombinant proteins (34). They are also easy to transfect and allow multiple copies of plasmid DNA to stably integrate into the genome (34). This property results in high levels of protein production which make them so attractive to use. The S2 cell line is derived from late stage *Drosophila* melanogaster embryos (35, 34). Schneider, the creator, described them as macrophage-like (34) and evidence for their immune lineage includes the following: (i) they undergo phagocytosis (34); (ii) produce antibacterial proteins (34); (iii) like mammalian macrophages prefer media with more carbonate (34), and (iv) will phagocytize other dying S2s.

Another reason why S2 cells present an attractive target for protein expression is related to the possibility of finely regulating protein expression through the use of vectors with strong, inducible promoters (34, 44). Another contributing factor to the use of S2 cells in this study was the prevalence of multiple isoforms of Orai and Stim genes in mammalian cells. Humans alone have three Orais: Orai1, Orai2 and Orai3; and two STIMs: STIM1 and STIM2 In contrast, S2 cells have only one Orai (dOrai) and one STIM (dSTIM). There are other advantages to using the *Drosophila* S2 cell line as well. The lack of response to high K^+ makes S2's good for transient or stable expression of ionotropic receptors (9). S2s also lack major contaminating currents from other channel types (44, 33).

The S2 cell population is known to display stable behavior over time (3). As with other immortalized cells, they can be frozen and used at later times. Another advantage is that it is possible to follow the responses of a population immediately after adding a drug (3). The addition of genes, either transiently or stably has been well documented. It is possible to do so quickly and easily. The silencing of gene function by RNA interference (RNA_i) is also relatively simple and well characterized in these cells (33). All of these factors make the *Drosophila* Expression System (DES) very attractive to work with.

In our studies we will be introducing genes and testing their function. Ultimately, our goal is to generate stable cell lines expressing our mammalian genes, and use this system for the purpose of drug discovery. DES also allows for fine grained control of genes of interest (GOI) by using appropriate promoters to drive gene expression. In our system, we have selected the metallothionein promoter to drive expression of our GOIs in a regulated fashion. The introduction of mammalian ion channels and receptors using such a system has been demonstrated previously (34, 18, 1, 20, 28).

1.5 Metallothionein

The *Drosophila* metallothionein (Mtn) promoter is a strong inducible promoter (34, 7, 26, 44). Experimentally Cu^{2+} at concentrations $\geq$ 500 μM will strongly activate Mtn; with basal activity being reported as close to undetectable (34). At the concentrations of Cu^{2+} that will induce the Mtn promoter, S2 cells can grow and make proteins (34).

1.6 Chemical reagents used

1.6.1 2-Aminoethoxyphenyl Borate

2-aminoethoxyphenyl borate (2-APB) (CAS Number: 524-95-8, $(C_6H_5)_2BOCH_2CH_2NH_2$) is a drug which has multiple effects on a variety of cellular organelles. It is an inhibitor of IP3Rs, SERCA pumps, and has both activating and inhibitory effects on channels (30, 6, 10). Its ability to activate and inhibit Orai channels will be exploited in this study. Its effect on Orai1 channels is to activate them at concentrations of 5 μM, while inhibiting at concentrations of 30 $_\mu$M or greater (16, 15). This dual effect is limited to Orai1, whereas for Orai3, 2-APB only activates at concentrations $\geq$ 50 μM (16).

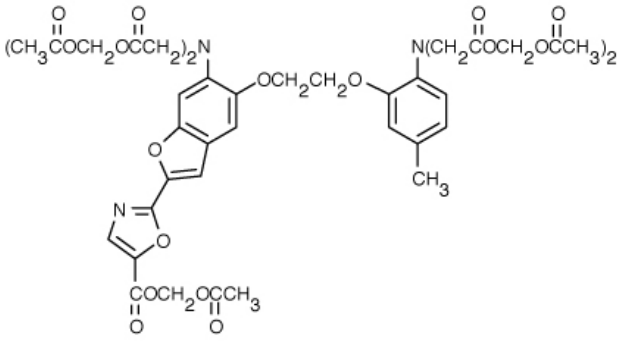

(a) Fura2-AM

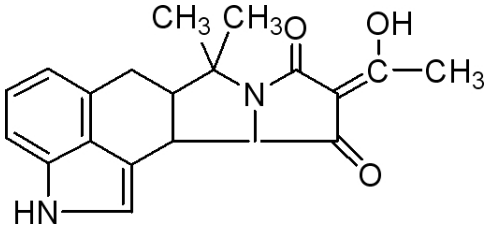

(b) CPA

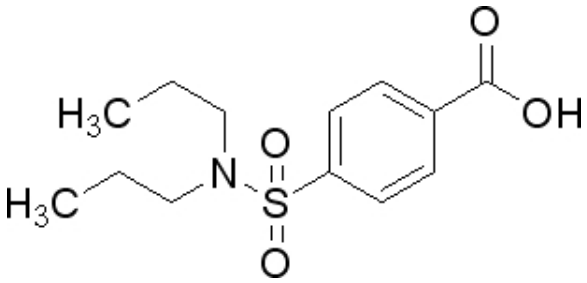

(c) Probenecid

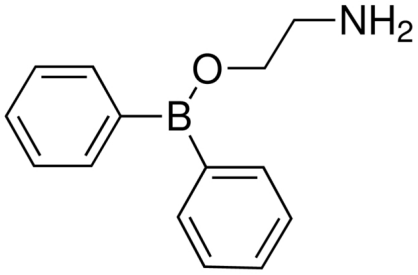

(d) 2-APB

Figure 1.1: Structures of chemical reagents used in this study.

1.6.2 Cyclopiazonic Acid

Cyclopiazonic Acid (CPA) (CAS Number: 18172-33-3, $C_{20}H_{20}N_2O_3$) is a specific inhibitor of the endoplasmic reticulum's Ca^{2+} ATPase (27). It has only been shown to inhibit the ER Ca^{2+} ATPase (SERCA Pump), and has been shown not to affect other ATPases or calcium pumps (27). The affinity of CPA for its substrate is 120 nM. The use of CPA allows for manipulation of SERCA pumps and by extension the ER Ca^{2+} store (32, chap. 2). Inhibition of the SERCA pump by CPA leads to release of the ER Ca^{2+} pools typically under the control of IP3R, (32, chap. 2). The SERCA pump inhibition reveals a persistent Ca^{2+} leak from the ER, and makes it the predominant force driving Ca^{2+} movement. The result is an increase of cytoplasmic Ca^{2+} as Ca^{2+} leaks from ER into cytoplasm. Ca^{2+} release occurs relatively quickly, as CPA is membrane permeant (32).

CPA is added in a Ca^{2+} free solution containing a Ca^{2+} chelator. We then switch to a solution that contains Ca^{2+}, with no CPA. By emptying the cell's intracellular stores first,

we may then reasonably assume that any subsequent increase in $[Ca^{2+}]_i$ is the result of Ca^{2+} coming into the cell from the external solution.

1.6.3 Ethylene glycol tetraacetic acid

Ethylene Glycol Tetraacetic Acid (EGTA) is a cation chelator with a preference for Ca^{2+} over Mg^{2+}, Na^{+} and K^{+} (19). It is used experimentally to bind available Ca^{2+} in the extracellular solution, making it unavailable for entry into the cell. This ensures that when $[Ca^{2+}]_i$ increases are seen during perfusion with a solution containing EGTA, we can assume that these increases are the result of intracellular Ca^{2+} release, rather than extracellular Ca^{2+} entry (19, 32).

1.6.4 Fura-2

The ability to measure $[Ca^{2+}]_i$ changes comes from our use of Fura-2. Fura-2 is a calcium indicator whose ability to bind calcium is the result of a tetracarboxylic acid core. It is a BAPTA derivative, which in turn, is based on EGTA's structure (19, 32).

Fura-2 is a dual excitation indicator with a Kd of 145 nM for Ca^{2+}. At low $[Ca^{2+}]$ excitation peaks at approximately 370 nm, while binding Ca^{2+} changes the excitation peak to 340 nm. Emission, meanwhile, is monitored at 510 nm. This results in Ca^{2+} binding leading to an increase in fluorescence at 510nm, when Fura-2 is excited at 340 nm. There is a corresponding decrease in fluorescence at 510 nm, when excited at 380 nm if Ca^{2+} is bound. By exciting both wavelengths in quick succession, Ca^{2+} binding changes can be monitored. This is referred to as a ratiometric approach, and has advantages over single wavelength excitation (discussed in 19).

The advantages are that the signal is not dependent on the dye concentration, illumination intensity or optical path-length because we get normalized values from the ratios of the two wavelengths. Dye leakage and photobleaching both lead to a loss of indicator

during the experiment. The ratiometric measurements are therefore an improvement over the single wavelength readings with respect to these issues as well. In a single wavelength setup, the dye concentration would gradually decrease, leading to a seeming decrease in Ca^{2+} signal. In the ratiometric setup, the effect of dye leakage or photobleached signals is mitigated by taking the ratios of these measurements. The ratios should remain constant regardless of the dye concentration or signal intensity. As an added bonus, ratiometric measurements also increase sensitivity. (19).

One noteworthy drawback is that Fura-2 fluorescence can be quenched by Cu^{2+} (32, 26). Since we use $CuSO_4$ to induce gene expression in S2 cells, this is directly relevant to our study. Care therefore is taken with measurements from $CuSO_4$-induced S2 cells. These cells are spun down, washed in PBS, and then resuspended in S2 media containing no $CuSO_4$ to minimize quenching.

Fura-2-AM

Ca^{2+} indicators are, necessarily, charged molecules. In spite of this, we them to cross the lipophilic PM. Since diffusional transport of these large, charged molecules across the lipophilic membrane would be extremely slow, other methods are used to speed up the process. By esterification of the -COOH groups of Fura-2, these groups are made lipophilic and thus membrane permeant. Indicators with these modifications already made are usually available as acetoxymethyl (AM) esters. Such is the case here, and the Fura-2-AM variant is used to load the dye into our S2 cells. Once inside the cells, cytosolic esterases are needed to remove the AM groups. Once these groups are removed, Fura-2 regains its charge, and may no longer freely cross the PM.

One caveat of this method is that cell types with poor esterase activity will display poor loading (19). Another is that cellular processes, presumably designed to maintain ionic equilibrium, may pump the de-esterified, charged compound out of the cell. To combat this problem, the anion transporters responsible for this process can be blocked. This strategy

was found to be necessary for S2 cells (9). Probenecid was used for this purpose in our study.

1.6.5 Probenecid

Probenecid (CAS Number: 57-66-9, $C_{13}H_{19}NO_4S$) is a nonspecific inhibitor of anion transport (9, 24). The reason for wanting to inhibit anion transport is to prevent cells from transporting the Fura-2 dye out of the cytosol. Many cell types are capable of sequestering the dye into different compartments, and also of transporting the dye out of the cell (11). There are a number of methods proposed for how Fura-2's cytosolic concentration could be reduced (11, 9). Of those, the hypothesis that anion transporters, which probenecid would block, is responsible seems most plausible in *Drosophila* S2 cells (9). Killer T-cells and murine macrophages have also shown a propensity for Fura-2 leakage (11). In the mouse macrophage model, the anion transporters were again been implicated in Fura-2 leakage and blocking anion transport in mouse macrophages prevented Fura-2 sequestration and secretion (11). It is easy to see then that S2 cells, which are also from an immune lineage (34), would have a similar response.

Drosophila S2 cells have, in fact, been shown to exhibit this problem with poor loading of Fura-2; one alleviated by the addition of probenecid (9). In our experiments we also experienced similar difficulties with loading the S2 cells in the absence of an anion blocker. Addition of 2.5 mM of probenecid alleviated this problem, increasing the number of cells loaded with Fura-2.

The mode of action of Probenecid

Probenecid is thought to act by inhibiting the clearance of ions (24). It has also been reported that the drug has non-specific effects, among them an altering of the Ca homeostasis (24). Such information is important to be aware of, as Ca^{2+} measurements are the output

from the experiments in our study. Care needs to be taken then, to ensure that the Ca^{2+} measurements would not be affected by probenecid. We address this by doing short 45-minute incubations in probenecid similar to other published studies (33, 9), followed by washing these cells in our perfusion solution without probenecid.

Probenecid is soluble at alkali basic pH. It is therefore dissolved in a solution of NaOH. This necessitates titrating the dye loading solution back to the desired pH, after adding probenecid (11). In mouse macrophage experiments, no unexpected effects on cell viability after a *3 hr* incubation with probenecid were observed (11). While there are caveats to its use, incubation at room temperature and for short periods, does not appear to affect cell viability or function (11, 9, 45).

1.7 Specific Aims

Before attempting to characterize Orai3 Ca^{2+} channels in *Drosophila* S2 cells, we needed to create the insect vector which contained our mammalian GOI. Standard molecular biology techniques were used to achieve this. The pharmacological characterization was done by measuring the effect of 2-Aminoethoxyphenyl Borate (2-APB) on heterologously expressed Orai3 activity. We hypothesized that gene expression of mammalian Orai3 in *Drosophila* S2 cells would result in Ca^{2+} channels that behave similar to those in mammalian cells expressing Orai3 genes, when administered with 2-APB.

1.7.1 Specific Aim #1

As mentioned earlier, *Drosophila* S2 cells provide a good system for expressing proteins from other organisms. The `pucHygroMT` vector was chosen to express our mammalian genes in S2 cells. Specific aim #1 is to create vector constructs using `pucHygroMT` which express Orai3 and STIM1 in *Drosophila* S2 cells.

1.7.2 Specific Aim #2

After creating these vector constructs it will be necessary to determine if they are capable of expressing the desired genes. Specific aim #2 is to show that we can successfully express heterologous genes in *Drosophila* S2 cells.

1.7.3 Specific Aim #3

It is our desire to ultimately use this system for drug discovery. For this to be possible we need to assess the effects which different drugs have in our system. This will be done using Ca^{2+} measurements taken in transfected *Drosophila* S2 cells. Specific aim #3 is to determine whether 2-APB has the same effect on the heterologously expressed Orai3 in S2s that it has in mammalian cells. 2-APB is a pharmacological agent with defined effects on the Orai3 Ca^{2+} channel. By looking at the effect of 2-APB on heterologously expressed Orai3, we will be able to determine whether the model requires refinement, or is suitable as is.

1.8 Significance

As stated above, Orai3 Ca^{2+} channels have been implicated in a specific subset of breast cancer. It is tempting to envision a scenario where we can specifically target a breast cancer for treatment (10). This will require some way to test the efficacy of drugs being used, however. If successful, creating a model system in *Drosophila* has the possibility to simplify drug testing, and as a result speed the process up. This could benefit research of, not only breast cancer, but also other diseases affected SOCE Ca^{2+}. Cancers, such as leukemia, and even autoimmune diseases such as rheumatoid arthritis or lupus, arising from defects of the immune system stand to benefit from this work.

Materials and Methods

2.1 Materials

Table 2.1: List of Cloning Reagents

Manufacturer	Item	Location
5 Prime	PerfectPrep EndoFree Plasmid Maxi Kit	Gaithersburg, MD
	Agarose Gelextract Mini Kit	
Agilent Technologies	Easy-A One-Tube RT-PCR Kit	Santa Clara, CA
Ambion	TRI Reagent®	Austin, TX
Fermentas	DNase I, RNase-free	Glen Burnie, MD
IBI Scientific	Ethidium Bromide (EtBr)	Peosta, IA
Invitrogen	MAX Efficiency® DH10β Competent cells	Carlsbad, CA
Lucigen	2.5 mM dNTP Mix	Middleton, WI
	EconoTaq PLUS GREEN 2X Master Mix	
Promega	PureYield™ Plasmid Miniprep System	Madison, WI
Research Products	Agarose	Mount Prospect, IL
International (RPI)	Tryptone	
	Yeast Extract	
New England Biolabs	Antarctic Phosphatase	Ipswich, MA
	T4 DNA Ligase	
	Various restriction enzymes	

2.1.1 Restriction enzymes

The following is a list of the restriction enzymes used. All were purchased from NEB:(i) SalI; (ii) XbaI; (iii) NruI; (iv) BamHI; (v) StuI; (vi) XhoI; (vii) ApaI; and (viii) KpnI.

Table 2.2: List of PCR Cloning Primers

Primer	Sequence
Orai3 start salI	TGCCGAGTCGACATGAAGGGCGGCGAGGGG
Orai3 end xbaI	TGCCGATCTAGATCACACAGCCTGCAGCTCCCC
Stim1 start salI	TGCCGAGTCGACATGGATGTATGCGTCCGTC
Stim1 end xbaI	TGCCGATCTAGAGCCTACTTCTTAAGAGGCTTCTT

Table 2.3: List of RT-PCR Primers

Primer	Sequence	Size
orai3_rtpcr_fwd	GAGTGACCACGAGTACCCACC	
orai3_rtpcr_rev	GGGTACCATGATGGCTGTGG	508 bp
hstim1_end_fwd	TTGGATTCTTCCCGTTCTCACAGC	
hstim1_rev	GCCTACTTCTTAAGAGGCTTCTT	228 bp
rp49-fwd	ATCGGTTACGGATCGAACAA	
rp49-rev	GACAATCTCCTTGCGCTTCT	165 bp
HygBP3	CCTGAACTCACCGCGACGTCTGTCG	
HygBP4	AGGCAGGTCTTGCAACGTGACACC	303 bp

2.1.2 Primers

All primers were purchased from Integrated DNA Technologies (Coralville, IA).

Table 2.4: List of Cell Culture Reagents

Manufacturer	Item	Location
Atlanta Biologicals	Fetal Bovine Serum - catalog no. S11050	Lawrenceville, GA
Lonza	Schneider's Drosophila Medium	Walkersville, MD

2.1.3 *Drosophila* resources

Drosophila Schneider line 2 (S2) cells, the `pucHygroMT` plasmid and the `puc18-act-gfp` plasmid were all purchased from the Drosophila Genomics Resource Center (Bloomington, IN). Figure 2.1 shows a schematic of the `pucHygroMT` vector, with possible sites of insertion in the MCS.

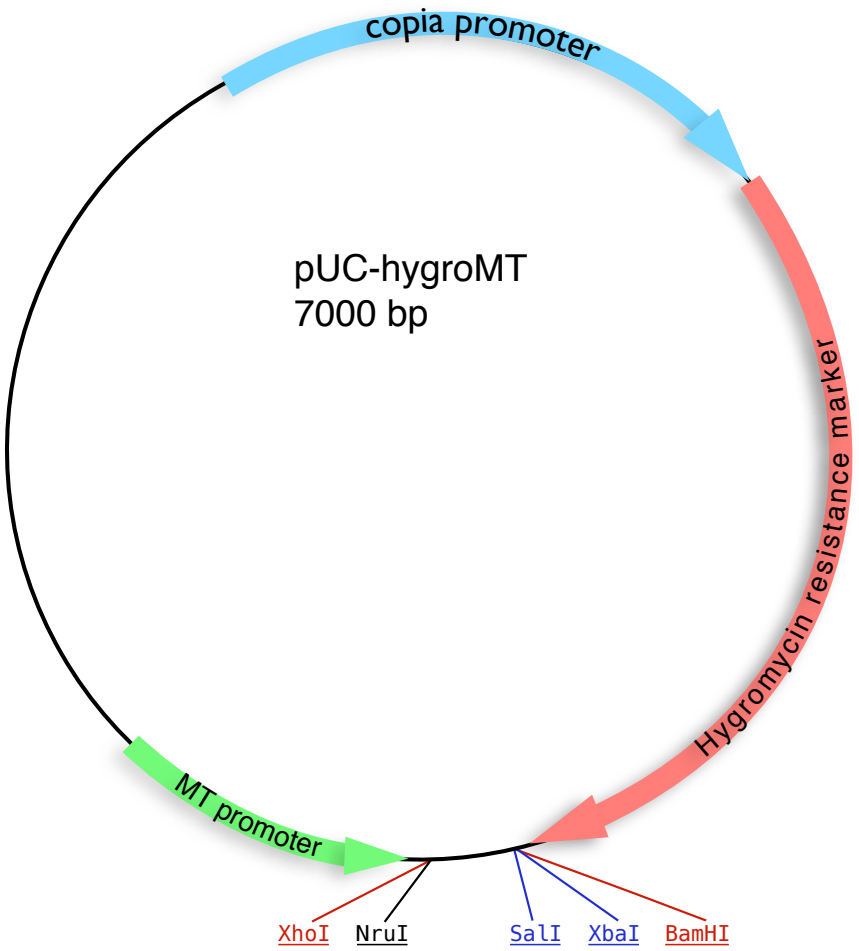

Figure 2.1: **Map of the `pucHygroMT` vector.** `pucHygroMT` contains `SalI` and `XbaI` sites which were used to insert both Orai3 and STIM1 into the MCS.

Table 2.5: List of Chemical Reagents

Manufacturer	Item	Location
Acros Organics	Ethylene Glycol Tetraacetic Acid (EGTA)	NJ
	4-(2-hydroxyethyl)-1-piperazineethanesulfonic	
	acid (HEPES)	
	HEPES Sodium Salt (HEPES-Na)	
	Paraformaldehyde 96%	
	Sodium Chloride (NaCl)	
Fisher Scientific	Cupric Sulfate Pentahydrate ($CuSO_4 \cdot 5H_2O$)	Fair Lawn, NJ
	Dimethyl Sulfoxide (DMSO)	
	D-glucose	
	Hydrochloric Acid (HCl) 10N	
	Potassium Chloride (KCl)	
	Sodium Hydroxide (NaOH) 10N	
Invitrogen	Fura-2 AM	Carlsbad, CA
Mirus Bio LLC	*Trans*IT®-2020 Transfection Reagent	Madison, WI
MP Biomedicals	Agar	Solon, OH
	Probenecid	
Sigma-Aldrich	2-Aminoethyl diphenylborinate (2-APB)	St. Louis, MO
	Cyclopiazonic Acid (CPA)	
	Pluronic® F-127	
	Fluka Analytical 1.0 M $CaCl_2$	
	Fluka Analytical 1.0 M $MgCl_2$	

Table 2.6: List of Instruments

Manufacturer	Item	Location
Applied Biosystems	2720 Thermal Cycler	Foster City, CA
Denver Instruments	UltraBasic pH/mV meter	Bohemia, NY
Sutter Instrument	Lambda 10-B	Novato, CA
Thermo Fisher Scientific	NanoDrop ND 1000	Wilmington, DE
Intracellular Imaging Inc.	175 W Xenon Lamp	Cincinnati, OH
B & B Microscopes, Ltd.	Olympus CKX41 Inverted Microscope	Pittsburgh, PA

2.2 Methods

2.2.1 Maintenance of cell lines

Drosophila S2 cells were cultured at 27 °C in Schneider's *Drosophila* medium supplemented with 10% fetal bovine serum (FBS).

2.2.2 Creation of *Drosophila* expression constructs

Molecular Cloning

We needed to express mammalian genes (Orai3, Stim1) on a *Drosophila* background, a process which required some molecular biology finesse. We chose to accomplish this by transferring these genes to a *Drosophila* vector. We selected the `pucHygroMT` plasmid as our vector, whereas Orai3 and Stim1 were the kind gifts of Dr. Stefan Feske, NYU School of Medicine.

`pucHygroMT` (see figure 2.1) contains a metallothionein promoter before the multiple cloning site (MCS), allowing for the induction of expression of genes placed in the MCS. It also provides the necessary genes for driving constitutive hygromycin B resistance. Also, `pucHygroMT` was available at a significantly lower cost compared to alternative vectors from commercial suppliers. Additionally, the use of this vector for induction and creation of stable lines has previously been documented (12).

Our genes of interest – mammalian Orai3 and Stim1 – were placed in the `pucHygroMT` plasmid using `SalI` and `XbaI` sites. The inserts for our genes of interest were created by polymerase chain reaction (PCR) using the primers listed in Table 2.2. The `Orai3 start salI` and `Orai3 end xbaI` primers were used for the Orai3 insert. The Stim1 insert was generated using `Stim1 start salI` and `Stim1 end xbaI` primers. The forward primer for each insert contained a `SalI` restriction site (**`GTCGAC`**), preceded by an `NruI` restriction site (**`TGCCGA`**). The reverse primer for each insert had an

XbaI restriction site (**TCTAGA**), preceded by an NruI restriction site (**TGCCGA**).

Each PCR reaction consisted of: (i) 1X Easy-A reaction buffer; (ii) .2 mM dNTPs; (iii) 2 μM forward; and (iv) 2 μM reverse primers; (v) 2 μL Easy-A PCR enzyme; (vi) 50-100 ng of template DNA; and (vii) nuclease-free water up to 100 μL.

The PCR reaction thermocycler parameters for each amplicon were as follows:

Orai3, (i) an initial denaturation step at 95 °C for 3 minutes; (ii) 27 cycles of denaturation at 95 °C for 40 seconds, followed by annealing at 65 °C for 30 seconds, then extension at 72 °C for 1 minute; and (iii) a final extension of 72 °C for 7 minutes.

Stim1, (i) an initial denaturation step at 95 °C for 3 minutes; (ii) 27 cycles of denaturation at 95 °C for 40 seconds, followed by an annealing step at 65 °C for 30 seconds, then extension at 72 °C for 130 seconds; and (iii) a final extension of 72 °C for 7 minutes were performed.

After the PCR reactions were completed, the amplicons were digested with SalI and XbaI, then ligated into a similarly digested pucHygroMT vector (see details below).

Engineering *Drosophila* vector contructs

Each PCR product and the pucHygroMT vector were digested by SalI and XbaI restriction enzymes. The vector digest was followed by treatment with Antarctic Phosphatase, according to the manufacturer's instructions. Phosphatase treatment removed the 5′ phosphate group at the end of the digested vector DNA. This helped prevent spontaneous recircularization and increased the amount of vector available to ligate with the insert. The digested vector and digested PCR amplicons were run on a 0.8% 1X TAE agarose gel for 90 minutes at 80 V. Following electrophoresis, the DNA band was excised under UV illumination. The vector and insert DNA were then purified using the Agarose GelExtract Mini kit. After purifying the DNA, a ligation reaction was performed with T4 DNA ligase following the manufacturer's specifications. The insert to vector ratios in the ligations were 9:1 (by volume). After a 15 minute incubation at 25 °C, the ligation mixture was used to

transform DH10β competent cells. The ligated constructs were renamed to indicate the inserts, thus pucHygMT-Orai3 contained Orai3, while pucHygMT-STIM1 contained Stim1.

Transformation of ligated DNA

A 15 ml round-bottom tube was chilled on ice, prior to addition of 100 μL thawed DH10β cells. Subsequently, 4 μL of the ligation mixture was added, mixed gently by flicking, then chilled on ice for 30 minutes. Next, the tube was incubated at 42 °C for 45 seconds, then quickly transferred to ice for 90 seconds. After this, 900 μL of SOC medium was added. A one hour incubation at 37 °C followed, with shaking at 250 RPM. 200 μL of this transformation mixture was plated on LB-Agar plates containing 100 μg/mL of the antibiotic ampicillin (+Amp). The resulting LB-Agar +Amp plates were placed in an incubator at 37 °C overnight. After 16-18 hrs the plates were transferred to 4 °C. Individual colonies from these plates were used to start miniprep cultures and obtain plasmid DNA.

Minipreparation of plasmid DNA

Single colonies were picked and added to 4 ml of LB supplemented with 100 μg/mL of ampicillin. This mixture was placed in an incubator at 37 °C, with shaking at 250 rpm, for 16-18 hours. A miniprep procedure was performed according to the instructions provided with the Pureyield™ Plasmid Miniprep System. DNA concentrations were estimated using a NanoDrop ND 1000 spectrophotometer.

Maxipreparation of plasmid DNA

A maxiprep culture consisting of 100 ml of LB, supplemented with 100 μg/ml of ampicillin was started, using 100 μL of the miniprep culture. This mixture was placed in an incubator at 37 °C, with shaking at 250 rpm, for 16-18 hours. A maxiprep procedure was

performed according to the protocol of the PerfectPrep EndoFree Plasmid Maxi kit. DNA concentrations were estimated using a NanoDrop ND 1000 spectrophotometer.

2.2.3 Transfection of S2 cells

S2 cells were transfected with *Trans*IT®-2020 transfection reagent according to the manufacturer's instructions. Briefly, one day prior to transfection, S2 cells were plated at 80% confluency in a 6-well tissue culture plate. `pucHygMT-Orai3` vector transfections were done with 1 μg of DNA per well. Transfections involving `pucHygMT-STIM1` used 2 μg of DNA per well. `pucHygMT-STIM1` and `pucHygMT-Orai3` co-transfections were performed at a 2:1 ratio (Stim1:Orai3).

As a positive control for transfection, 0.25 μg of the green fluorescent protein (GFP) vector `puc18-act-gfp`, was co-transfected with the above constructs. A ratio of 3 μL of *Trans*IT®-2020 was used per 1 μg of maxiprepped DNA.

Induction of transfected S2 cells with $CuSO_4$

Drosophila S2 cells were induced by the addition of 750 μM $CuSO_4$ one or two days post-transfection.

2.2.4 RT-PCR and cDNA synthesis

Total RNA was isolated from transfected S2 cells, two days post-induction, using TRI reagent® as per the manufacturer's instructions. Traces of contaminating DNA were removed using RNase-free DNase I. For each μg of RNA, 1 μL of DNase I was added. First strand cDNA synthesis was performed using the MMLV reverse transcriptase (RT). Briefly, 1 μg of mRNA was reverse transcribed into cDNA during a 30 minute incubation at 45 °C. This cDNA served as the template for successive PCR reactions.

The RT reaction mixture contained: (i) 1X MMLV buffer; (ii) .8 mM dNTPs; (iii) 1 μg of template RNA; (iv) 2 μL MMLV RT; and (v) nuclease-free water up to 50 μL. RT reactions were also performed on samples with the RT omitted – to determine whether any contaminating DNA was still present.

PCR reactions were performed in a 2720 Thermal Cycler. The *Drosophila* housekeeping gene, ribosomal protein 49 (rp49), was used as a positive control to determine whether cDNA was made in the preceding RT reaction (7, 23).

Each PCR reaction contained: (i) 1x Easy-A reaction buffer; (ii) .3 mM dNTPs; (iii) 1 μM forward; and (iv) 1 μM reverse primers; (v) .5 μL Easy-A PCR enzyme; (vi) 5 μL of cDNA template from the (no-)RT reaction; and (vii) nuclease-free water up to 50 μL. The sequences of these RT-PCR primers (23, 25, 43), and expected band sizes are given in Table 2.3.

The PCR reaction parameters are as follows:

Orai3 and Stim1, (i) an initial denaturation step at 95 °C for 3 minutes; (ii) 30 cycles of denaturation at 95 °C for 30 seconds, then annealing at 55 °C for 30 seconds, then extension at 72 °C for 1 minute; and (iii) a final extension of 72 °C for 10 minutes was performed.

HygBP, (i) an initial denaturation step at 95 °C for 3 minutes; (ii) 30 cycles of denaturation at 95 °C for 30 seconds, then annealing at 65 °C for 30 seconds, then extension at 72 °C for 30 seconds; and (iii) a final extension of 72 °C for 10 minutes was performed.

rp49, (i) an initial denaturation step at 94 °C for 3 minutes; (ii) 30 cycles of denaturation at 94 °C for 45 seconds, then annealing at 50 °C for 1 minute, then extension at 72 °C for 1 minute 30 seconds; and (iii) a final extension of 72 °C for 7 minutes was performed.

2.2.5 Ca^{2+} imaging experiments

Two primary solutions were used for the Ca^{2+} imaging experiments. The first, designated **2 Ca**, contained (in mM): 2 $CaCl_2$, 4 $MgCl_2$, 150 NaCl, 5 KCl, 10 HEPES and, 10 D-glucose

at pH 7.2 (48). The second solution **1 EGTA**, contained (in mM), 1 EGTA, 6 $MgCl_2$, 150 NaCl, 5 KCl, 10 HEPES and, 10 D-glucose at pH 7.2 (48). The dye loading solution referred to below was comprised of 2 Ca, 0.02% Pluronic F-127, 2.5 mM probenecid and 4 μM Fura2-AM.

Cytosolic Ca^{2+} signals were measured in the following way: S2 cells, cultured at 27 °C, were placed in 35 mm glass-bottom chambers made by J. Ashot Kozak, Ph. D. After 30 minutes at room temperature, the old medium was removed, and the cells washed in 1X DPBS twice. After the wash, the dye-loading solution was added to the cells and they were incubated at room temperature for 45 minutes. The cells were then washed twice with the 2 Ca solution, and used for imaging.

Ca^{2+} imaging was performed on the stage of an Olympus CKX41 inverted microscope, attached to a Dell Optiplex 745C computer. Cells were perfused at a rate of approximately 4 mL/min using the solutions indicated in the figures below. Loaded cells were exposed to light of 340 nm and 380 nm wavelengths, and emitted light at 510 nm was recorded. The UV light source was a 175 W Xenon arc lamp. The wavelengths were selected using filters in the Lambda 10-B SmartShutter which was controlled by the InCytIM 2 software (Intracellular Imaging, Cincinnati, OH).

Selection of data for analysis

The traces were selected based on the following criteria: (i) there was a visible response to CPA introduction; (ii) the initial perfusion with 2 Ca was relatively stable over time; (iii) the absolute values of the measurements at 340 nm and 380 nm were $\geq$ 40 during initial perfusion with 2 Ca; and (iv) the 340 nm and 380 nm recordings mirrored each other as time progressed.

Statistical analysis of imaging experiment data

Error bars shown on the traces depict the standard error of the mean. Area under the curve analysis was performed using Origin 8 software. Statistical analysis of the area under the curve data was performed using one way ANOVA with SAS software. Differences were considered significant if p values were < 0.05. The p values of < 0.001 were denoted by the *** characters.

Results

GGGGATCTCGAGCTCGCGAAAGCTTGCATGCCTGCAGGTCGAC

ATGAAGGGCGGCGAGGGGGACGCGGGCGAGCAGGCCCCGCTGAACCCTGAGGGCGAGAGC

CCTGCAGGCTCGGCCACGTACCGGGAGTTCGTGCACCGCGGCTACCTGGACCTCATGGGG

GCCAGTCAGCACTCGCTGCGGGCGCTCAGCTGGCGCCGCCTCTACCTCAGCCGGGCCAAG

CTCAAAGCTTCCAGCCGCACGTCTGCCTTGCTCTCGGGCTTCGCCATGGTGGCCATGGTG

GAGGTGCAGCTGGAGAGTGACCACGAGTACCCACCAGGCCTGCTGGTGGCCTTCAGTGCC

TGCACCACCGTGCTGGTGGCTGTGCACCTCTTTGCACTCATGGTCTCCACGTGTCTGCTG

CCCCACATTGAAGCTGTGAGCAACATCCACAACCTCAACTCTGTCCACCAGTCGCCACAC

CAGAGACTGCACCGCTACGTGGAGCTGGCCTGGGGCTTCTCCACTGCCCTGGGCACCTTT

CTCTTCCTTGCTGAAGTTGTCCTGGTTGGTTGGGTCAAGTTTGTGCCCATTGGGGCTCCC

TTGGACACACCGACCCCCATGGTGCCCACATCCCGGGTGCCCGGGACTCTGGCACCAGTG

GCTACCTCCCTTAGTCCAGCTTCCAATCTCCCACGGTCCTCTGCGTCTGCAGCACCGTCC

CAGGCTGAGCCAGCCTGCCCACCCCGGCAAGCCTGTGGTGGTGGTGGGGCCCATGGGCCA

GGCTGGCAAGCAGCCATGGCCTCCACAGCCATCATGGTACCCGTGGGGCTCGTGTTTGTG

GCCTTTGCCCTGCATTTCTACCGCTCCTTGGTGGCACACAAGACAGACCGCTACAAGCAG

GAACTAGAGGAACTGAATCGCCTGCAGGGGGAGCTGCAGGCTGTGTGA

TCTAGAGGATCCGCGGCCGCCCTCGACGGATCCAGACATGATAAGATACATT

3.1 Creating inducible vectors

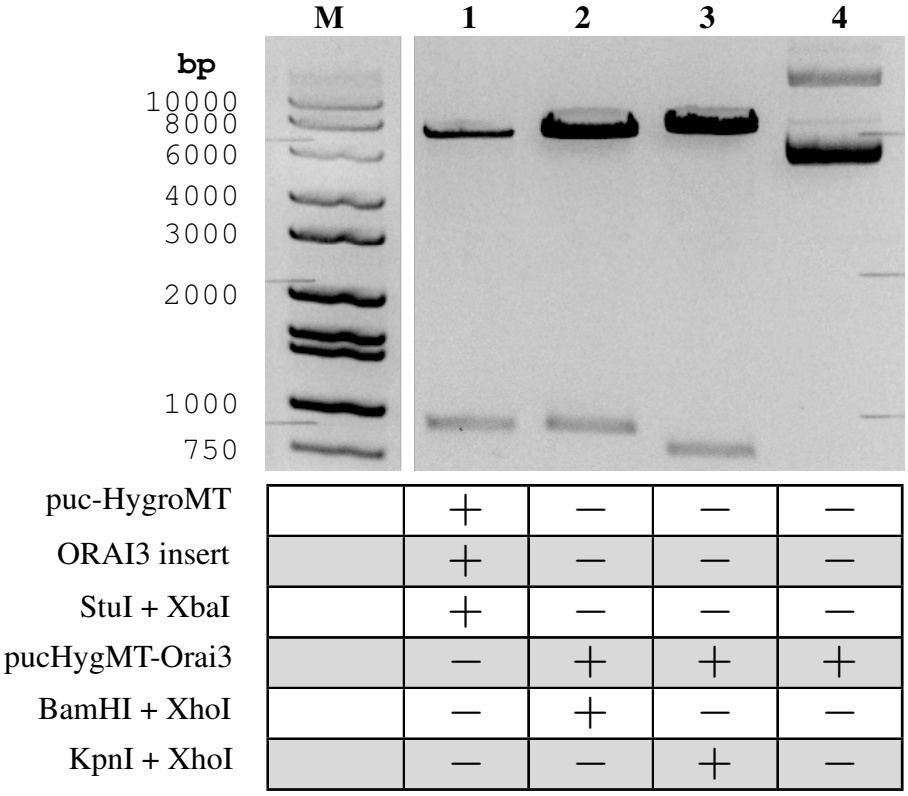

Figure 3.1: **Restriction digests confirm the insertion of Orai3 into puc-HygroMT**. **Lane M** shows the DNA ladder, with the sizes of the corresponding bands to their left. **Lane 1** shows a `SalI+XbaI` double digest of both `pucHygroMT` and the Orai3 PCR amplicon. The double digested `pucHygroMT`, ∼7000 bp in size, is the higher of the two bands. Orai3, which is 894 bp in size, is the lower band. **Lane 2** shows the result of a `BamHI+XhoI` double digest of `pucHygMT-Orai3`. The complete vector is ∼7888 bp. From a 931 bp fragment and the remainder of the vector, ∼6957 bp. **Lane 3** shows the result of a `KpnI+XhoI` double digest of `pucHygMT-Orai3`. This gives a 796 bp band and a remaining ∼7092 bp band. **Lane 4** shows the undigested `pucHygMT-Orai3`. This yields supercoiled and open circular vector DNA species.

After ligating the `pucHygroMT` and inserts and transforming the products, the DNA obtained from the maxipreparation was digested to confirm that the desired constructs were generated. Figure 3.1 shows the results of digesting the `pucHygMT-Orai3` construct after electrophoresis on a 0.8% 1X TAE gel. The marker lane, shows DNA bands of known sizes, used for estimating the sizes of bands in subsequent lanes. In lane 1 shows the sizes

obtained when both pucHygroMT vector and the Orai3 PCR amplicon are digested with SalI+XbaI. The pucHygroMT vector map gives its size as 7000 bp. Based on comparison with the DNA marker, double digested pucHygroMT is estimated to be ∼7000 bp. This implies a difference of only a few bases between the SalI and XbaI sites in the MCS. The Orai3 PCR amplicon, after digestion, is 894 bp. This comes from the 888 bp size of Orai3, plus the bases for the digested SalI and XbaI restriction sites. A reasonable estimate for the size of pucHygMT-Orai3 would be 7888 bp. This comes from the ∼7000 bp size of the digested vector and the 888 bp Orai3 insert. The restriction sites in the Orai3 amplicon are not added to the total, as they are already accounted for in the vector.

We tested whether insertion of pucHygMT-Orai3 was successful by doing restriction digests and comparing the estimated size of the obtained bands, with the size that was expected. The double digest of pucHygMT-Orai3 with BamHI and XhoI is shown in lane 2 of figure 3.1. Digestion with these enzymes is expected to yield a 931 bp and ∼6957 bp bands. Observed bands are approximately this size, based on comparison with our DNA marker, and the digested DNA in lane 1. Our 931 bp band is at roughly the same point as the 894 bp Orai3 insert, and both are just below the 1000 bp marker.

For the pucHygMT-Orai3 construct we tested whether our insert was placed in the correct orientation by digesting with an enzyme which cut the vector, and an enzyme which cut the insert . Lane 3 of figure 3.1 shows the result of a KpnI and XhoI double digest of pucHygMT-Orai3. This time we see the ∼7888 bp vector producing the expected 796 bp and ∼7092 bp bands.

The last lane shows us what the undigested pucHygMT-Orai3 looks like. We are therefore able to observe the supercoiled and open circular DNA species of the vector in lane 4. Taken together, figure 3.1 shows that Orai3 was inserted into pucHygroMT, and more importantly, in the correct direction. Further confirmation was obtained after sequencing pucHygMT-Orai3.

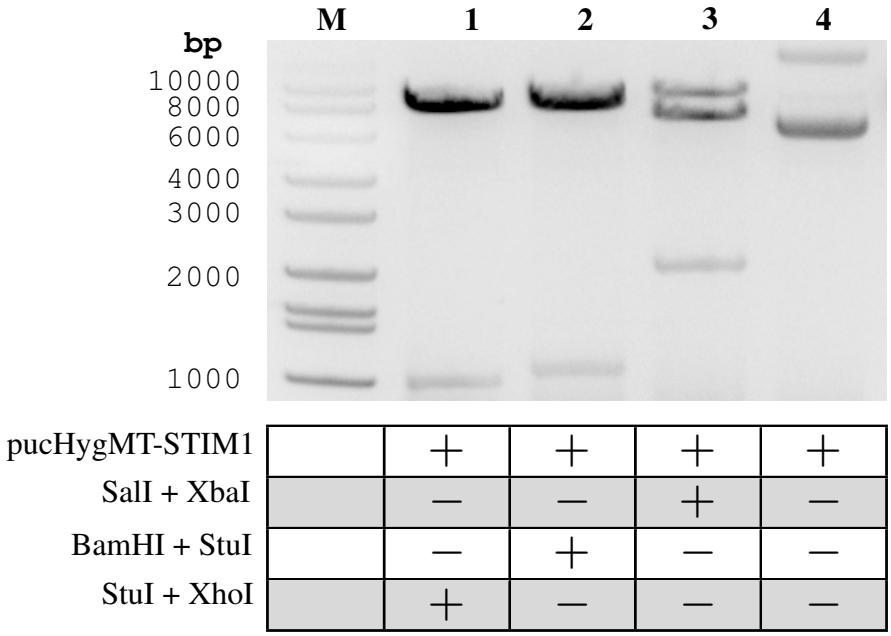

Figure 3.2: **Restriction digests confirm the insertion of STIM1 into puc-HygroMT**. **Lane 1** shows a `StuI+XhoI` digest of `pucHygMT-STIM1`. The ∼7000 bp `puc-HygroMT` and 2060 bp STIM1 create a ∼9060 bp construct. `StuI+XhoI` digestion gives 1016 bp and ∼8044 bp bands. **Lane 2** shows the result of a `BamHI+StuI` digest of `pucHygMT-STIM1`. This yields 1087 bp and ∼7973 bp bands. **Lane 3** is the `SalI+XbaI` digest of `pucHygMT-STIM1`. A 2066 bp band and a ∼6994 bp band are the result. Linearized `pucHygMT-STIM1`, at ∼9060 bp is also present. **Lane 4** shows the undigested `pucHygMT-STIM1`. We see supercoiled and open circular vector DNA species here.

We again confirmed successful creation of our STIM1 construct with restriction digests. Figure 3.2 shows the results of `pucHygMT-STIM1` digests after electrophoresis on a 0.8% 1X TAE agarose gel. Again, the marker lane shows DNA of known sizes, and is used to estimate the band size in subsequent lanes.

In lane 1 the `StuI+XhoI` digest provides confirmation of STIM1 insertion into `pucHyg-MT-STIM1`. The `StuI` site is specific to STIM1 while the `XhoI` site is specific to the vector. Two bands, sized at approximately 8044 bp and 1016 bp were expected and obtained. In lane 2 the `StuI` and `BamHI` digest provide additional confirmation of properly inserted STIM1. In this digest reaction `BamHI` is present only in the vector. This digest yields the anticipated bands at approximately 7973 bp and 1087 bp. Insertion of STIM1

in the reverse direction would have yielded different sizes. These results confirm that our insert is present, and further, in the desired orientation. We can see that our gel is also able to resolve the difference between 1016 bp and 1087 bp (though not between 1016 bp and 1000 bp) providing further confirmation that our inserts are oriented correctly.

The `SalI` and `XbaI` digest in lane 3 further supports our claims. The 2066 bp STIM1 and ∼6994 bp vector fragments are visible. A third band, the linearized `pucHyg-MT-STIM1` vector, is also visible at ∼9060 bp. That the ∼8 kb (7973 bp) band in lane 2, fits between our expected ∼7 kb and ∼9 kb bands in lane 3 also supports our assertion that `pucHygMT-STIM1` contains STIM1 in the desired orientation. Lane 4 shows undigested `pucHygMT-STIM1` with supercoiled and open circular DNA species.

3.2 Demonstrating inducible expression

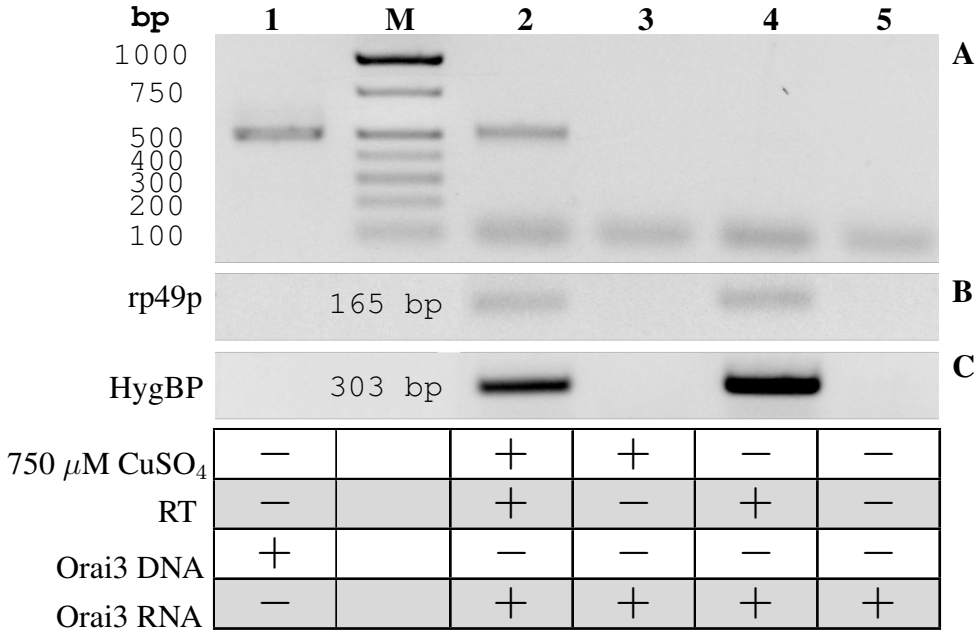

Figure 3.3: **Orai3 expression is inducible in *Drosophila* S2 cells using 750 μM $CuSO_4$.** (**A**) In **lanes 1-5** the Orai3 RT-PCR primer pair are used (see table 2.3) **Lane 1** shows the band from a positive control PCR reaction. Orai3 DNA is used as the template. **Lanes 2-5** show RT-PCRs using RNA from isolated `pucHygMT-Orai3` transfected S2 cells. **Lanes 2-3**: S2 cells were induced with 750 μM $CuSO_4$. 508 bp band only present when RT is added. **Lane 4-5**: S2 cells were not induced with $CuSO_4$. No band present after RT-PCR. (**B**) RT-PCR of the same samples as in A, using rp49 primers. We see rp49 bands at 165 bp only in the lanes where RT was added to the reaction. (**C**) RT-PCR of the same samples as in A, with HygBP primers. HygBP bands at 303 bp are seen only in the lanes where RT was added to the reaction.

The RT-PCR reactions in figure 3.3 were performed on RNA collected from `pucHygMT-Orai3`-transfected (Orai3+) S2 cells. Figure 3.3 shows that induction of Orai3 RNA in these S2 cells is successful. Panel A shows that DNA positive control and RNA induction bands are the same size, 508 bp. No observable band is present when $CuSO_4$ is not added to Orai3+ S2 cells in lanes 4 and 5. This suggests negligible levels of Orai3 gene expression when under control of the metallothionein promoter.

Panels B shows rp49 RNA present in equal amounts for Orai3+ cells with or without $CuSO_4$. The rp49 RT-PCR looks for expression of the housekeeping gene rp49, and serves as a positive control for RT-PCR from Orai3+ S2s. Panel C shows more HygBP RNA in Orai3+ S2 cells with no $CuSO_4$ added. This is suggestive of a pipeting error occurring. Panels A, B and C all showed no evidence of DNA contamination of these RT-PCR reactions, as lanes where RT was omitted (indicated in table) did not produce bands.

Some lower bands were observed in all the RT-PCR reactions and are likely the result of primer-dimer products. Such phenomenon has been documented elsewhere (8).

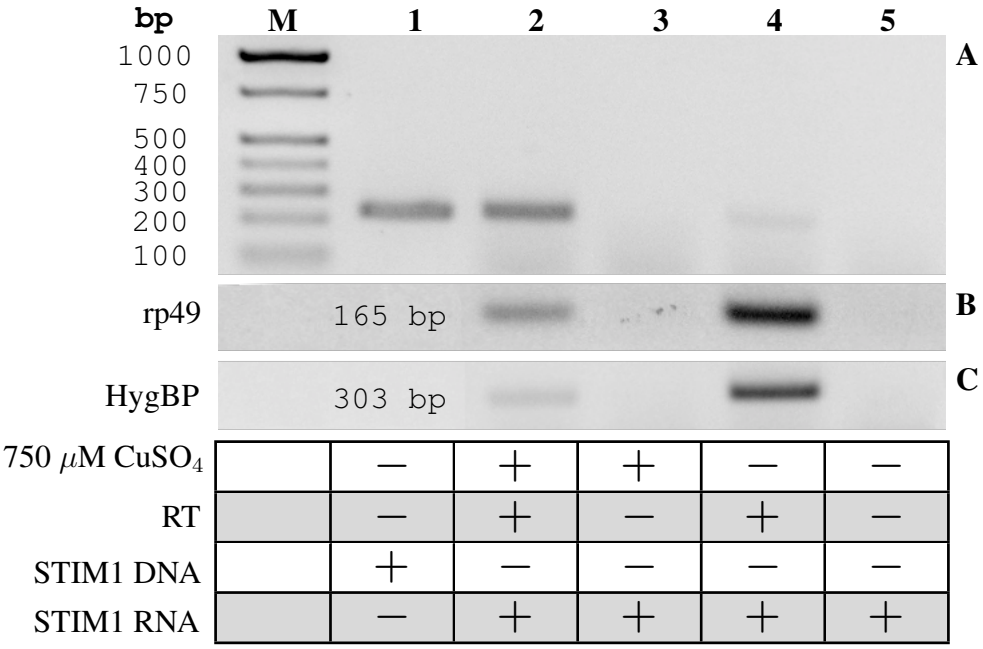

Figure 3.4: **STIM1 expression is inducible in *Drosophila* S2 cells using 750 μM $CuSO_4$** (**A**) In **lanes 1-5** the STIM1 RT-PCR primer pair are used (see table 2.3). **Lane 1** shows the positive control PCR band using STIM1 template DNA. **Lanes 2-5** show RT-PCRs using RNA from isolated `pucHygMT-STIM1` transfected S2 cells. **Lanes 2-3**: S2 cells induced with 750 μM $CuSO_4$. 228 bp band present only when RT added. **Lanes 4-5**: S2 cells not induced with $CuSO_4$. Faint band at 228 bp seen when RT added. (**B**) RT-PCR using rp49 primers yields bands only in the lanes with RT added. (**C**) RT-PCR using HygBP primers yields bands only in the lanes where RT added.

The RT-PCR reactions in figure 3.4 were performed on RNA collected from `pucHyg-MT-STIM1`-transfected (STIM1+) S2 cells. Figure 3.4 shows that induction of STIM1 RNA in these S2 cells is successful. Panel A shows that DNA positive control and RNA induction bands are the same size. Both show up in the region where we would expect to see a 228 bp band. A faint band in the uninduced STIM1 RT-PCR reaction is visible in lane 4 of panel A. This suggests a basal level of expression for STIM1 when under the control of the metallothionein promoter.

Panels B and C show that more RNA was present in RT-PCR reactions of uninduced STIM1+ S2 cells, when compared to RNA from $CuSO_4$ induced STIM1+ S2 cells. This was present in both panels B and C, suggesting an error in estimating the RNA concentra-

tion using the NanoDrop spectrophotometer. This adds further support for the successful induction of STIM1 RNA from $CuSO_4$ induced STIM1+ cells. More RNA was present in the *uninduced* RT-PCR reactions, yet a much brighter STIM1 band was present in the $CuSO_4$ induced lane.

There was no evidence of DNA contamination of the RT-PCR reactions, as lanes without RT, produced no bands.

3.3 Effective measurement of Ca^{2+} transients

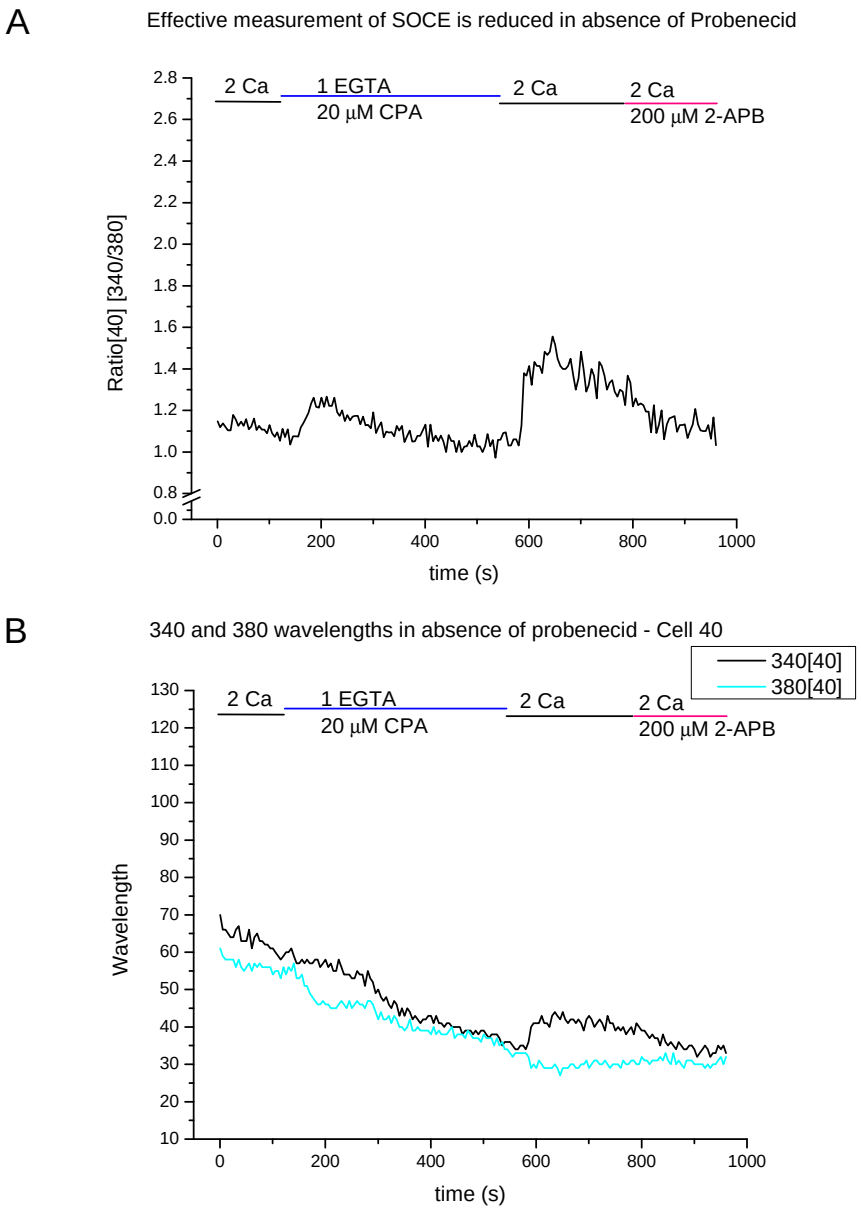

Figure 3.5: **The absence of probenecid results in poor Ca^{2+} imaging results in S2 cells**. (**A**) The ratio of the 340 nm and 380 nm wavelengths of an individual cell during the course of one perfusion experiment where probenecid was omitted from the incubation solution. (**B**) The individual 340 nm and 380 nm wavelength values, which produced the ratio seen in **A**.

Figure 3.5A shows a recording from an individual S2 cell which was loaded without probenecid present in the dye-loading solution (DLS). Figure 3.5B shows the individual 340 and 380 nm wavelength values that produced the trace in 3.5A. Though the trace of the ratio hides it, we see that both wavelengths values start decreasing immediately after the start of the experiment. The decreasing values continues to the end of the experiment. This figure illustrates the leakage of Fura-2 which takes place in S2 cell if probenecid is absent in the DLS. The Ca^{2+} ratios reported after SOCE, upon reintroduction of 2 Ca is also shown to be low here. This is an artifactual recording caused by less Fura-2 being around to bind to Ca^{2+}, thereby limiting the amount of Ca^{2+} which can be measured in the cytosol.

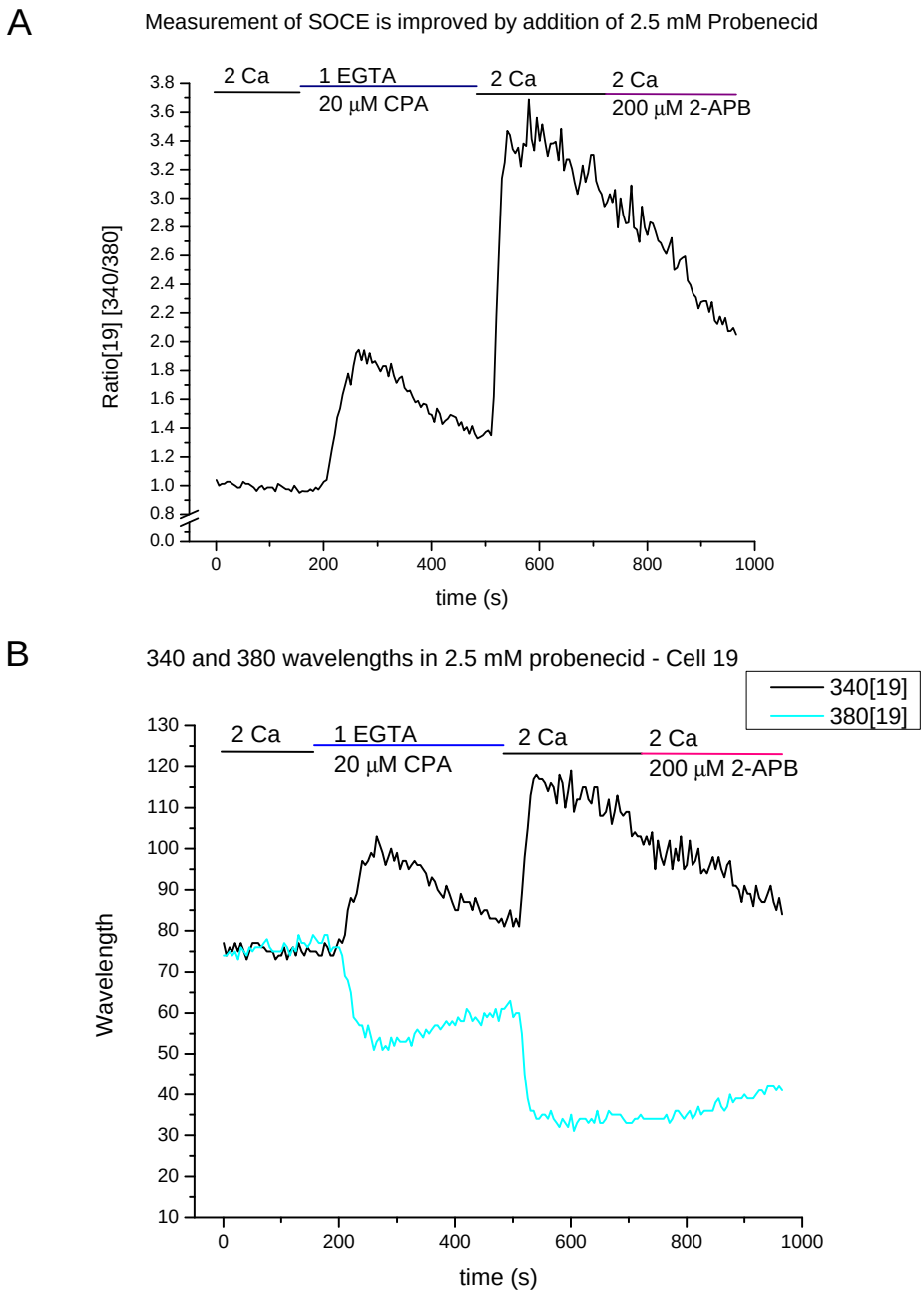

Figure 3.6: **The presence of 2.5 mM probenecid results in much improved Ca^{2+} imaging in S2 cells**. (**A**) The ratio of the 340 nm and 380 nm wavelengths of an individual cell during the course of a perfusion experiment where 2.5 mM probenecid was included in the incubation solution. (**B**) The individual 340 nm and 380 nm wavelength values, which produced the ratio seen in **A**.

Figure 3.6A shows a sample recording from a cell incubated with DLS containing 2.5 mM probenecid. The ratio is robust and provides better resolution than the trace in figure 3.5. Figure 3.5B gives the individual 340 nm and 380 nm wavelengths which were used to obtain the ratio in 3.5A. We are able to clearly see the reciprocal nature of the 340 nm and 380 nm wavelength values. The steady decline of the values over the course of the experiment is no longer apparent. Probenecid has stopped or greatly slowed leakage of Fura-2 from the cytosol. As a result, we are able to record higher Ca^{2+} transients as more Fura-2 is available as the experiment proceeds, compared to cells loaded without probenecid. This is readily apparent in the SOCE portion of the trace.

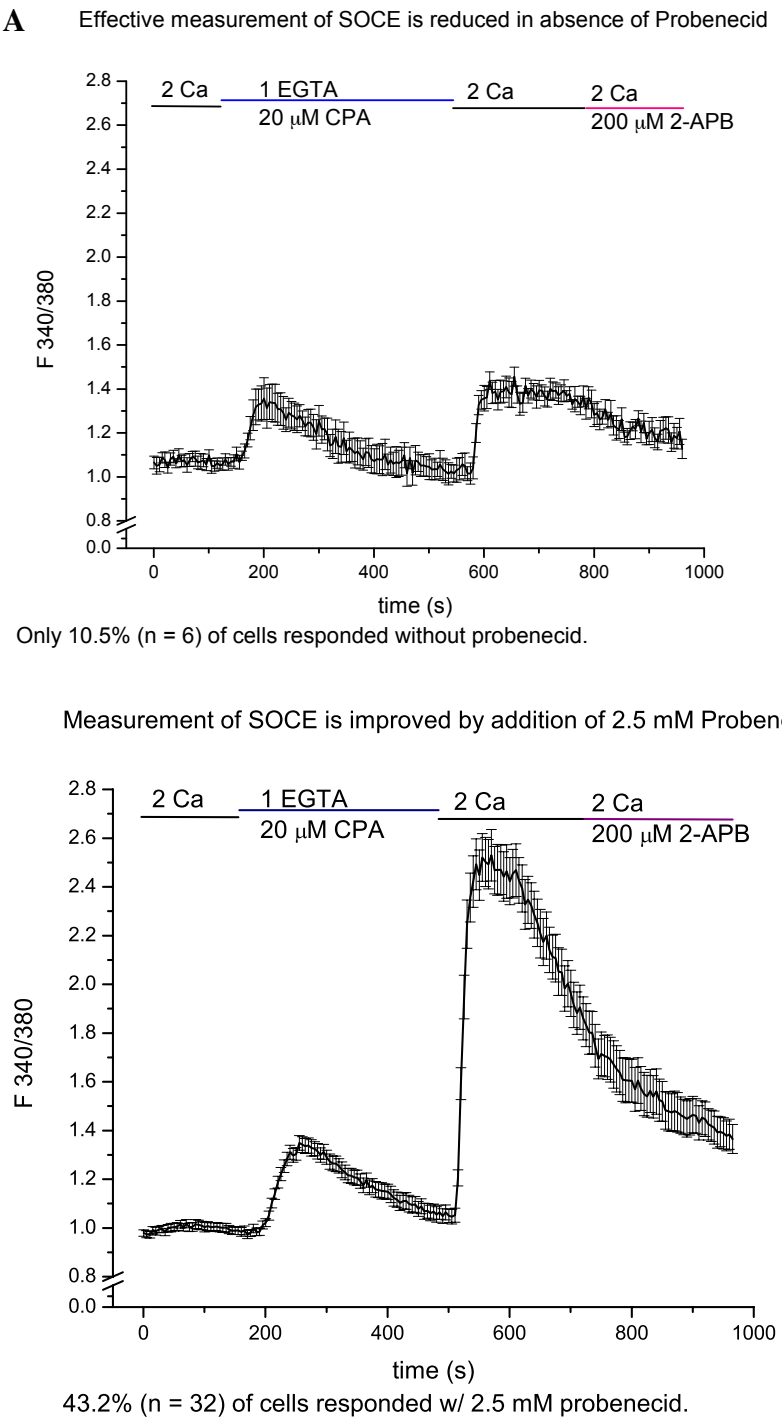

Figure 3.7: **Addition of Probenecid improves Ca^{2+} recordings**. (**A**) Recordings taken from a population of cells incubated in dye-loading solution that did not contain probenecid (**B**) Recordings taken from a population of cells incubated in dye-loading solution that contained 2.5 mM probenecid.

Figure 3.7 shows a population of cells loaded without (3.7A) and with (3.7B) probenecid. We are able to observe a larger Ca^{2+} transient, due to more Fura-2 being available. Also, addition of probenecid results in more cells meeting the selection criteria for data collection. This can be attributed to Fura-2 retention in probenecid treated S2 cells. The result is more dye being available at the start of the experiment, and as it progresses.

Unhealthy cells, cells with damaged or otherwise compromised plasma membranes may also be omitted from the data set in a reliable, unbiased manner after probenecid treatment. Such cells would still display characteristics of cells not treated with probenecid, such as pronounced, constant dye leakage.

Conditions for selecting data were formulated after looking at the individual 340 nm and 380 nm wavelength values for probenecid treated, and probenecid untreated cells. Three out of six of the cells in figure 3.7A, had either 340 nm or 380 nm wavelength values below 40. This led to 40 being used as a cutoff value for selecting data. For the S2 cells selected, both the 340 nm or 380 nm wavelength values stayed at or above 40 during the initial 2 Ca perfusion. This allowed for elimination of cells which were leaky, even after treatment with probenecid which, for reasons explained above, were deemed undesirable.

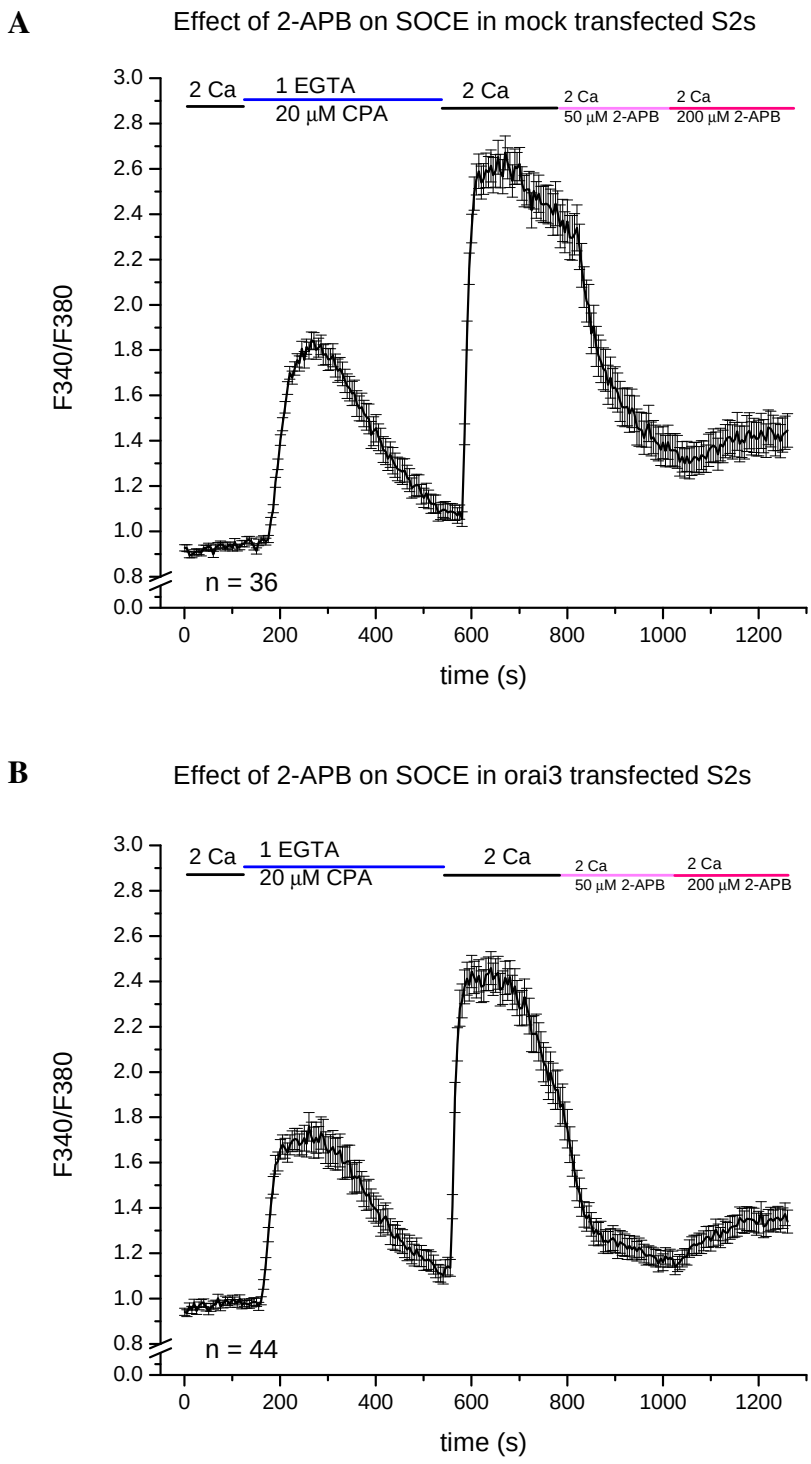

Figure 3.8: **Ca^{2+} measurements in transfected S2 cells perfused with 2-APB**. The lines above the trace are labeled with the solutions perfused during those times. **A**) Sample trace of mock transfected S2s showing the effect of 2-APB on SOCE. **B**) Sample trace of Orai3 transfected S2s showing the effect of 2-APB on SOCE.

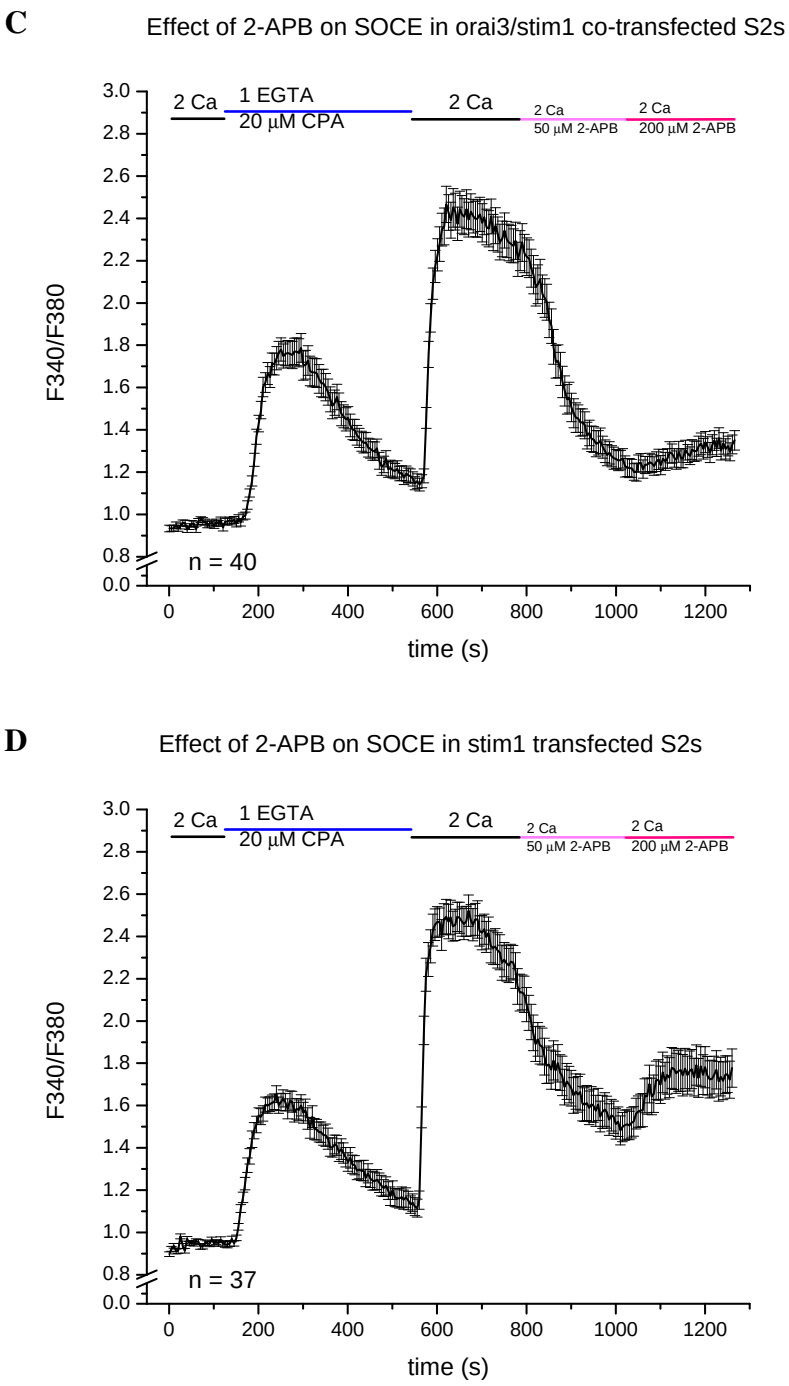

Figure 3.8: **Ca^{2+} measurements in transfected S2 cells perfused with 2-APB**. The lines above the trace are labeled with the solutions perfused during those times. **C**) Sample trace of Orai3+STIM1 transfected S2s showing the effect of 2-APB on SOCE. **D**) Sample trace of STIM1 transfected S2s showing the effect of 2-APB on SOCE.

The composite in figure 3.8 shows representative traces for Ca^{2+} imaging experiments where S2 cells have been mock transfected or transfected with Orai3, STIM1, or Orai3+STIM1. In figure 3.8A we see a sample trace giving the result of an experiment on mock transfected S2s. Initially, the 2 Ca perfusion of these mock transfected S2s is relatively stable. Upon introduction of 20 μM CPA in 1 EGTA, we observe an increase in the F340/F380 ratio. This indicates an increase in cytosolic free Ca^{2+}, resulting from leakage of Ca^{2+} from the ER. This Ca^{2+} leak achieves a maximum and subsequently declines. The decline phase is indicative of Ca^{2+} being pumped out of the cell, shuttled to non-ER compartments, such as the mitochondria, or being bound by cytosolic Ca^{2+} chelators. Transport of Ca^{2+} to the ER is prevented by CPA, which blocks the necessary SERCA pumps.

After 7 minutes of perfusion in 1 EGTA/20 μM CPA, Ca^{2+} is reintroduced with the 2 Ca solution. The mock transfected S2s then undergo SOCE, and a second Ca^{2+} transient forms at this stage. The maximal Ca^{2+} entry after 2 Ca reintroduction is greater than maximal Ca^{2+} release from the ER. The *dOrai* channels responsible for SOCE in S2 cells are able to open quickly, allowing Ca^{2+} into the cell shortly after switching to the 2 Ca solution. We eventually begin to see less Ca^{2+} recorded, which can be attributed to *dOrai* channels closing, slowing Ca^{2+} entry.

After 4 minutes in 2 Ca, 50 μM 2-APB is added to the perfusion solution. We see for the mock transfected S2 cells, that the gradual decline in Ca^{2+} measurements becomes sharper, shortly after addition of 2-APB. This is expected as because 2-APB is inhibitory at these concentrations, for *dOrai*. The decline in Ca^{2+} readings continue during the 4 minutes that the 50 μM 2-APB perfusion lasts.

After 4 minutes in 2 Ca with 50 μM 2-APB, the perfusion solution is changed to 2 Ca with 200 μM 2-APB. This solution was perfused across the cells for another 4 minutes and then the experiment was stopped. During this time we observe what seems to be a slight increase. The overlap of the error bars along the trace indicate that, while the trend of the trace tends toward an increasing nature, further analysis is required to determine what is

happening at this point. In order to address, the question of what happens to the Ca^{2+}, area under the curve analysis was performed on each 4 minute section after store-depletion occuredfor each transfected group.

Figure 3.8B shows a sample trace of an experiment on Orai3 transfected S2s. The initial and store-depletion phases are similar to those in the mock transfected S2s. 2 Ca reintroduction shows the swift onset of SOCE. The expected increase in Ca^{2+} after addition of 50 μM 2-APB is not seen, however. Addition of 200 μM 2-APB seemed to result in a marginal increase in Ca^{2+} entry. The Ca^{2+} content of this 200 μM 2-APB phase was analyzed further and found to not be a significant change from the mock (see figure 3.9).

As no distinct effect of 2-APB was observed in S2s transfected with only Orai3, Orai3+STIM1 transfections were performed. A sample trace for one of these experiments is provided in figure 3.8C. The store-depletion and SOCE phases again seem similar to that of the mock and Orai3 transfected cells. When treated with 50 and then 200 μM 2-APB, no clear trend was visible compared to the mock or Orai3 transfected cells.

In figure 3.8D a similar experiment was performed, but on STIM1 transfected S2s. Here, the store-depletion and SOCE phases after 2 Ca reintroduction are similar to mock and other transfections. Interestingly, addition of 50 μM 2-APB in the STIM1 only transfected cells, was less effective at slowing Ca^{2+} entry than in the other transfections. When 200 μ 2-APB was added, a clear increase in the cytosolic Ca^{2+} was observed.

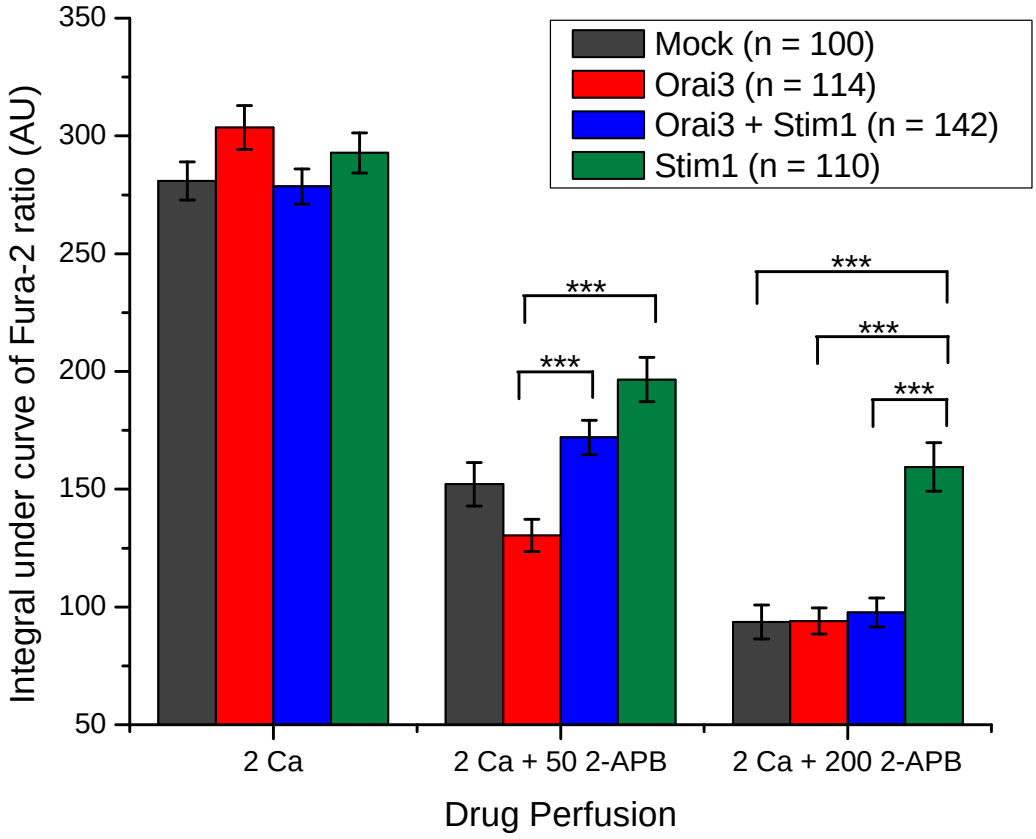

Figure 3.9: **Cytoplasmic Ca^{2+} content in transfected S2 cells**.

Figure 3.9 displays the results of area under the curve (AUC) analysis on the three phases of treatment after store-depletion. By doing AUC analysis, the ratios generated by Fura-2 recordings were translated into cytosolic Ca^{2+} content of arbitrary units. The three groups in the bar graph correspond to perfusion with 2 Ca, 2 Ca + 50 μM 2-APB, and 2 Ca + 200 μM 2-APB. The perfusion time for each group was 4 minutes. A one way ANOVA was used to determine if there were significant differences in the drug treatment groups. If significant differences were found, Tukey's studentized range test, was used to determine where significant differences lie between the transfection groups.

The 2 Ca group represents an untreated period of SOCE in the transfection groups. Statistical analysis showed no significant change in cytosolic Ca^{2+} for this group. Functional Orai3 Ca^{2+} channels were expected to increase the levels of cytosolic Ca^{2+} during

SOCE. That this was not observed may be due to the Ca^{2+} capacity of the cell already being at maximal levels. If the S2 cell is capable of holding a finite amount of Ca^{2+}, and it had already reached that point, more Ca^{2+} channels would merely get it to that point faster, but observing further increase in Ca^{2+} levels would not be expected in this case.

The 2 Ca + 50 2-APB experiments did show significant differences in this treatment group. Significant differences existed between Orai3+STIM1 transfected cells and the Orai3 only transfected group. There were also significant differences between STIM1 only transfected cells and Orai3 only transfected cells. For both of the groups described above, the Orai3 only group showed much less cytosolic Ca^{2+}, which was unexpected. A significant difference was also found between mock transfected and STIM1 transfected cells, with the STIM1 transfected group containing higher levels of cytosolic calcium than the mock transfected group. The significant differences for all of the above was $p < 0.0001$ at the 0.05 confidence level.

The 2 Ca + 200 2-APB showed significant differences only between the STIM1 transfected cells and all the other groups. Again, an unexpected result.

Discussion

As demonstrated in figures 3.1 and 3.2 the ligation of the inserts and subsequent cloning of `pucHygMT-Orai3` and `pucHygMT-STIM1` were successful. *Drosophila* vectors *capable* of expressing mammalian Orai3 and STIM1 genes in S2 cells were created, satisfying specific aim #1.

Figures 3.3 and 3.4 then showed induction of Orai3 and STIM1 *gene expression* from these vectors. This demonstrated that both vector constructs actually expressed these mammalian genes in *Drosophila* S2 cells, satisfying specific aim #2. Having carried out the objectives in specific aims #1 and #2, we moved on to address specific aim #3: assessing the effect of 2-APB on Orai3 channels. As mentioned previously concentrations of ≥ 50 μM 2-APB will activate mammalian Orai3 channels.

Initial attempts at taking Ca^{2+} measurements in S2 cells were thwarted by leakage of Fura-2, the ratiometric dye being used, from these cells. As demonstrated in figures 3.5, 3.6 and 3.7 addition of the anion transport inhibitor probenecid was crucial to recording satisfactory calcium transients. We see that omission of probenecid led to ratio measurements of SOCE transients which were lower than those recorded when probenecid was present. The lower ratio maxima for SOCE transients was the result of less Fura-2 being present for binding to Ca^{2+} due to a persistent leak. We see that addition of probenecid alleviated Fura-2 leakage by blocking the transporters responsible, and resulted in better measurements of S2 cell populations. This demonstrates that the use of probenecid for Ca^{2+} recordings of *Drosophila* S2 cells is necessary for obtaining quality data.

After solving the issue of recording Ca^{2+} transients, assessing the effect of 2-APB on S2 cells expressing Orai3 was possible. Our hypothesis, that gene expression of mammalian Orai3 in *Drosophila* S2s would result in Ca^{2+} channels that behaved similarly to those in mammalian cells expressing Orai3 proved incorrect. As seen by the results presented in figures 3.8 and 3.9, Orai3 channel behavior in our *Drosophila* expression system was anamalous. Aims #1 and two were achieved, but testing of aim #3 showed that the expression model required further refinement.

An unexpected and interesting result from this study was the ability of STIM1 to cause an increase in cytosolic Ca^{2+}. The results in figure 3.8 for the STIM1 only transfection hint at less *deactivation* of *dOrai* occurring in 50 μM 2-APB compared to the mock transfection. Addition of 200 μM 2-APB to STIM1 only transfected S2s resulted in a clear increase in cytosolic calcium indicative of channel opening. One explanation is that another Ca^{2+} channel opened due to the combination of STIM1 and 2-APB. It may also be that 200 μM 2-APB is interacting with STIM1 leading to non-specific effects on *dOrai*. As this is only present in the STIM1 transfected cells, and since STIM1 and Orai3+STIM1 transfected S2s have the same amount of STIM1 (2 μg) this suggests an effector+2-APB interaction in the absence of Orai3.

There are a few possibilities for why Orai3, either alone or with STIM1, did not display the expected Ca^{2+} increase after addition of 50 or 200 μM 2-APB. The most obvious is that while Orai3 RNA production was induced with $CuSO_4$, actual protein production did not occur. Another possibility is that the transfection efficiency was consistently low with the TransIT-2020 reagent and `pucHygMT-Orai3` DNA. This may have resulted in poor expression of Orai3 and a paucity of Orai3 protein translation, leading to a deficiency in Orai3 channels expressed at the cellular surface. Another possibility is that, because of how closely related Orai3 and *dOrai* are, Orai3 forms heterodimers with *dOrai*, and adopts a phenotype primarily *dOrai* in nature.

Given that STIM1 expression results in an unexpected phenotype, it is unlikely that

Orai3, the smaller protein which was made in a similar manner, does not express. It is more likely that interactions with the closely related *dOrai* result in heteromeric channels, and it is the output from those channels that we are investigating.

Transfection of Orai3 with STIM1 did lead to a significant increase in cytosolic Ca^{2+} compared to Orai3 only transfected cells (see figure 3.9). This suggests that *dStim* is not sufficient for Orai3 function.

Future work on this project will involve testing the possibilities presented above, for why Orai3 activation did not occur after 2-APB treatment. The generation of stable cell lines using the hygromycin B resistance conferred by `pucHygroMT` is underway. Stable lines expressing Orai3 and STIM1 will facilitate experiments needed to test these possibilities.

Protein expression of Orai3 can be tested by isolating proteins from transfected cells and performing a Western Blot using antibodies to Orai3. Testing for interference from native *dOrai* by performing RNA_i knockdown will address the issue of *dOrai* influencing the Orai3 channel phenotypes. These types of experiments are also beneficial because Orai3 Ca^{2+} channel function can be assessed on a *dOrai* free background. Beyond the potential issue of *dOrai* affecting Orai3 function and/or expression, RNA_i knockdown of *dOrai* allows study of only Orai3 channels without any contributions from *dOrai* channels. This will be useful for defining Orai3 channel function, as opposed to general SOCE channel function, to which Orai3 may contribute.

4.1 Conclusion

The creation of an expression system for mammalian Orai Ca^{2+} channels to be used for drug discovery purposes was begun in this study. The proteins selected to probe the feasibility of using such a system were the mammalian Orai3 Ca^{2+} channel, and mammalian Ca^{2+} sensor STIM1. Constructs which expressed in S2 cells were created and were able

to successfully express genes from both mammalian Orai3, and mammalian STIM1. The system was not able to reproduce the function of the Orai3 Ca^{2+}, in the presence of the known effector 2-APB, highlighting the need for further refinement, before use in future drug studies.

The system is effective in inducing the expression of Orai3 and STIM1, however, and is currently being used to generate stable cell lines to further this study. The system promises to be a very useful tool, for study of not just Orai3 channels, but the entire Orai family. Given the importance of SOCE to immune cells, and related disease states, this initial work and future studies based upon it, promise to be important vehicles for contributing to the body of knowledge in the field of Ca^{2+} entry. Study of diseases resulting from disrupted Ca^{2+} homeostasis including forms of cancer and autoimmune diseases may also benefit from the creation of this type of expression system.

Bibliography

1. ASMILD, M. AND WILLUMSEN, N. J. 2000. Chloride channels in the plasma membrane of a foetal Drosophila cell line, S2. *Pflügers Archiv : European journal of physiology 439,* 6, 759–64.

2. BAKSH, S. AND BURAKOFF, S. J. 2000. The role of calcineurin in lymphocyte activation. *Seminars in immunology 12,* 4, 405–15.

3. BAUM, B. AND CHERBAS, L. 2008. Drosophila cell lines as model systems and as an experimental tool. In *Drosophila: Methods and Protocols*, C. Dahmann, Ed. Vol. 420. Humana Press, Totowa, NJ, Chapter 25, 391–424.

4. BERRIDGE, M. J., BOOTMAN, M. D., AND RODERICK, H. L. 2003. Calcium signalling: dynamics, homeostasis and remodelling. *Nature Reviews Molecular Cell Biology 4,* 7, 517–529.

5. BERRIDGE, M. J., LIPP, P., AND BOOTMAN, M. D. 2000. The versatility and universality of calcium signalling. *Nature Reviews Molecular Cell Biology 1,* 1, 11–21.

6. BILMEN, J. G., WOOTTON, L. L., GODFREY, R. E., SMART, O. S., AND MICHELANGELI, F. 2002. Inhibition of SERCA Ca2+ pumps by 2-aminoethoxydiphenyl borate (2-APB). *European Journal of Biochemistry 269,* 15, 3678–3687.

7. BUNCH, T., GRINBLAT, Y., AND GOLDSTEIN, L. 1988. Characterization and use of the Drosophila metallothionein promoter in cultured Drosophila melanogaster cells. *Nucleic acids research 16,* 3, 1043–61.

8. CHUMAKOV, K. 1994. Reverse transcriptase can inhibit PCR and stimulate primer-dimer formation. *PCR Methods and Applications 4,* 1, 62–64.

9. CORDOVA, D., DELPECH, V. R., SATTELLE, D. B., AND RAUH, J. J. 2003. Spatiotemporal calcium signaling in a Drosophila melanogaster cell line stably expressing a Drosophila muscarinic acetylcholine receptor. *Invertebrate neuroscience 5,* 1, 19–28.

10. DELLIS, O., MERCIER, P., AND CHOMIENNE, C. 2011. The boron-oxygen core of borinate esters is responsible for the store-operated calcium entry potentiation ability. *BMC pharmacology 11,* 1, 1.

11. DI VIRGILIO, F., STEINBERG, T. H., AND SILVERSTEIN, S. C. 1990. Inhibition of Fura-2 sequestration and secretion with organic anion transport blockers. *Cell calcium 11,* 2-3, 57–62.

12. EBLE, J. A., WUCHERPFENNIG, K. W., GAUTHIER, L., DERSCH, P., KRUKONIS, E., ISBERG, R. R., AND HEMLER, M. E. 1998. Recombinant soluble human alpha 3 beta 1 integrin: purification, processing, regulation, and specific binding to laminin-5 and invasin in a mutually exclusive manner. *Biochemistry 37,* 31, 10945–55.

13. EID, J.-P., ARIAS, A. M., ROBERTSON, H., HIME, G. R., AND DZIADEK, M. 2008. The Drosophila STIM1 orthologue, dSTIM, has roles in cell fate specification and tissue patterning. *BMC developmental biology 8,* 1, 104.

14. FESKE, S., GWACK, Y., PRAKRIYA, M., SRIKANTH, S., PUPPEL, S.-H., TANASA, B., HOGAN, P. G., LEWIS, R. S., DALY, M., AND RAO, A. 2006. A mutation in Orai1 causes immune deficiency by abrogating CRAC channel function. *Nature 441,* 7090, 179–185.

15. GOTO, J.-I., SUZUKI, A. Z., OZAKI, S., MATSUMOTO, N., NAKAMURA, T., EBISUI, E., FLEIG, A., PENNER, R., AND MIKOSHIBA, K. 2010. Two novel 2-aminoethyl diphenylborinate (2-APB) analogues differentially activate and inhibit store-operated Ca(2+) entry via STIM proteins. *Cell calcium 47,* 1, 1–10.

16. GWACK, Y., SRIKANTH, S., FESKE, S., CRUZ-GUILLOTY, F., OH-HORA, M., NEEMS, D., HOGAN, P., AND RAO, A. 2007. Biochemical and functional characterization of Orai proteins. *Journal of Biological Chemistry 282,* 22, 16232–43.

17. HOTH, M. AND PENNER, R. 1992. Depletion of intracellular calcium stores activates a calcium current in mast cells. *Nature 355,* 6358, 353–356.

18. JOHANSON, K., APPELBAUM, E., DOYLE, M., HENSLEY, P., ZHAO, B., ABDEL-MEGUID, S., YOUNG, P., COOK, R., CARR, S., MATICO, R., AND OTHERS. 1995. Binding Interactions of Human Interleukin 5 with Its Receptor α Subunit. *Journal of Biological Chemistry 270,* 16, 9459–9471.

19. LAMBERT, D. G. 2006. *Calcium signaling protocols*, 2nd ed. Methods in molecular biology. Humana Press, Totowa, NJ.

20. LANSDELL, S. J., COLLINS, T., YABE, A., GEE, V. J., GIBB, A. J., AND MILLAR, N. S. 2008. Host-cell specific effects of the nicotinic acetylcholine receptor chaperone RIC-3 revealed by a comparison of human and Drosophila RIC-3 homologues. *Journal of neurochemistry 105,* 5, 1573–81.

21. LEWIS, R. S. 2001. Calcium signaling mechanisms in T lymphocytes. *Annual review of immunology 19,* Figure 1, 497–521.

22. LIOU, J., KIM, M. L., HEO, W. D., JONES, J. T., MYERS, J. W., FERRELL, J. E., AND MEYER, T. 2005. STIM is a Ca2+ sensor essential for Ca2+-store-depletion-triggered Ca2+ influx. *Current Biology 15,* 13, 1235–1241.

23. LUCE-FEDROW, A., VON OHLEN, T., BOYLE, D., GANTA, R. R., AND CHAPES, S. K. 2008. Use of Drosophila S2 cells as a model for studying Ehrlichia chaffeensis infections. *Applied and environmental microbiology 74,* 6, 1886–91.

24. MASEREEUW, R., VAN PELT, A., VAN OS, S., WILLEMS, P., SMITS, P., AND RUSSEL, F. 2000. Probenecid interferes with renal oxidative metabolism: A potential pitfall in its use as an inhibitor of drug transport. *British journal of pharmacology 131,* 1, 57–62.

25. MIGNEN, O., THOMPSON, J. L., AND SHUTTLEWORTH, T. J. 2008. Both Orai1 and Orai3 are essential components of the arachidonate-regulated Ca2+-selective (ARC) channels. *The Journal of physiology 586,* 1, 185–95.

26. MILLAR, N. S., BAYLIS, H. A., REAPER, C., BUNTING, R., MASON, W. T., AND SATTELLE, D. B. 1995. Functional expression of a cloned Drosophila muscarinic acetylcholine receptor in a stable Drosophila cell line. *The Journal of experimental biology 198,* Pt 9, 1843–50.

27. MONCOQ, K., TRIEBER, C. A., AND YOUNG, H. S. 2007. The molecular basis for cyclopiazonic acid inhibition of the sarcoplasmic reticulum calcium pump. *The Journal of biological chemistry 282,* 13, 9748–57.

28. PFEIFER, T. 1998. Expression of heterologous proteins in stable insect cell culture. *Current opinion in biotechnology 9,* 5, 518–21.

29. PRAKRIYA, M., FESKE, S., GWACK, Y., SRIKANTH, S., RAO, A., AND HOGAN, P. G. 2006. Orai1 is an essential pore subunit of the CRAC channel. *Nature 443,* 7108, 230–233.

30. PRAKRIYA, M. AND LEWIS, R. S. 2001. Potentiation and inhibition of Ca(2+) release-activated Ca(2+) channels by 2-aminoethyldiphenyl borate (2-APB) occurs independently of IP(3) receptors. *The Journal of physiology 536,* 1, 3–19.

31. PUTNEY, J. W. 1986. A model for receptor-regulated calcium entry. *Cell Calcium 7,* 1, 1–12.

32. PUTNEY, J. W. 2006. *Calcium signaling*, 2nd ed. Methods in signal transduction. CRC Press, Boca Raton, FL.

33. ROOS, J., DIGREGORIO, P. J., YEROMIN, A. V., OHLSEN, K., LIOUDYNO, M., ZHANG, S., SAFRINA, O., KOZAK, J. A., WAGNER, S. L., CAHALAN, M. D., VELIÇELEBI, G., AND STAUDERMAN, K. A. 2005. STIM1, an essential and conserved component of store-operated Ca2+ channel function. *The Journal of cell biology 169,* 3, 435–45.

34. SCHETZ, J. A. AND SHANKAR, E. P. N. 2004. Protein expression in the Drosophila Schneider 2 cell system. *Current protocols in neuroscience Chapter 4*, 4.16.1–15.

35. SCHNEIDER, I. 1972. Cell lines derived from late embryonic stages of Drosophila melanogaster. *Journal of embryology and experimental morphology 27,* 2, 353–65.

36. SMYTH, J., HWANG, S., TOMITA, T., DEHAVEN, W., MERCER, J., AND PUTNEY, J. 2010. Activation and regulation of store-operated calcium entry. *Journal of Cellular and Molecular Medicine 14,* 10, 2337–2349.

37. SOBOLOFF, J., SPASSOVA, M. A., HEWAVITHARANA, T., HE, L.-P., XU, W., JOHNSTONE, L. S., DZIADEK, M. A., AND GILL, D. L. 2006. STIM2 is an inhibitor of STIM1-mediated store-operated Ca2+ Entry. *Current Biology 16,* 14, 1465–1470.

38. STREB, H., IRVINE, R. F., BERRIDGE, M. J., AND SCHULZ, I. 1983. Release of Ca2+ from a nonmitochondrial intracellular store in pancreatic acinar cells by inositol-1,4,5-trisphosphate. *Nature 306,* 5938, 67–69.

39. TAYLOR, C. 2006. Store-operated Ca2+ entry: a STIMulating stOrai. *Trends in biochemical sciences 31,* 11, 597–601.

40. TIMMERMAN, L. A., CLIPSTONE, N. A., HO, S. N., NORTHROP, J. P., AND CRABTREE, G. R. 1996. Rapid shuttling of NF-AT in discrimination of Ca2+ signals and immunosuppression. *Nature 383,* 6603, 837–840.

41. VIG, M., PEINELT, C., BECK, A., KOOMOA, D. L., RABAH, D., KOBLAN-HUBERSON, M., KRAFT, S., TURNER, H., FLEIG, A., PENNER, R., AND KINET, J.-P. 2006. CRACM1 is a plasma membrane protein essential for store-operated Ca2+ entry. *Science 312,* 5777, 1220–3.

42. WILLIAMS, R., MANJI, S., PARKER, N., HANCOCK, M., VAN STEKELENBURG, L., EID, J., SENIOR, P., KAZENWADEL, J., SHANDALA, T., SAINT, R., SMITH, P. J., AND DZIADEK, M. A. 2001. Identification and characterization of the STIM (stromal interaction molecule) gene family: coding for a novel class of transmembrane proteins. *Biochemical Journal 357,* 3, 673–685.

43. XU, Y.-B., LI, H.-P., ZHANG, J.-B., SONG, B., CHEN, F.-F., DUAN, X.-J., XU, H.-Q., AND LIAO, Y.-C. 2010. Disruption of the chitin synthase gene CHS1 from Fusarium asiaticum results in an altered structure of cell walls and reduced virulence. *Fungal genetics and biology 47,* 3, 205–15.

44. YAGODIN, S., PIVOVAROVA, N. B., ANDREWS, S. B., AND SATTELLE, D. B. 1999. Functional characterization of thapsigargin and agonist-insensitive acidic Ca2+ stores in Drosophila melanogaster S2 cell lines. *Cell calcium 25,* 6, 429–38.

45. YEROMIN, A. V., ROOS, J., A STAUDERMAN, K., AND CAHALAN, M. D. 2004. A store-operated calcium channel in Drosophila S2 cells. *The Journal of general physiology 123,* 2, 167–182.

46. ZHANG, S. L., KOZAK, J. A., JIANG, W., YEROMIN, A. V., CHEN, J., YU, Y., PENNA, A., SHEN, W., CHI, V., AND CAHALAN, M. D. 2008. Store-dependent and

-independent modes regulating Ca2+ release-activated Ca2+ channel activity of human Orai1 and Orai3. *The Journal of biological chemistry 283,* 25, 17662–71.

47. ZHANG, S. L., YEROMIN, A. V., ZHANG, X. H.-F., YU, Y., SAFRINA, O., PENNA, A., ROOS, J., STAUDERMAN, K. A., AND CAHALAN, M. D. 2006. Genome-wide RNAi screen of Ca(2+) influx identifies genes that regulate Ca(2+) release-activated Ca(2+) channel activity. *Proceedings of the National Academy of Sciences of the United States of America 103,* 24, 9357–62.

48. ZHANG, S. L., YU, Y., ROOS, J., KOZAK, J. A., DEERINCK, T. J., ELLISMAN, M. H., STAUDERMAN, K. A., AND CAHALAN, M. D. 2005. STIM1 is a Ca2+ sensor that activates CRAC channels and migrates from the Ca2+ store to the plasma membrane. *Nature 437,* 7060, 902–905.

49. ZWEIFACH, A. AND LEWIS, R. S. 1993. Mitogen-regulated Ca2+ current of T lymphocytes is activated by depletion of intracellular Ca2+ stores. *Proceedings of the National Academy of Sciences of the United States of America 90,* 13, 6295–9.